

AD-A038 873

MASSACHUSETTS INST OF TECH CAMBRIDGE DEPT OF OCEAN E--ETC F/6 20/4  
HYDRODYNAMICS OF CYLINDERS IN WATER OF ARBITRARILY VARYING DEPT--ETC(U)  
MAY 76 Y KIM

N00014-75-C-0236

NL

UNCLASSIFIED

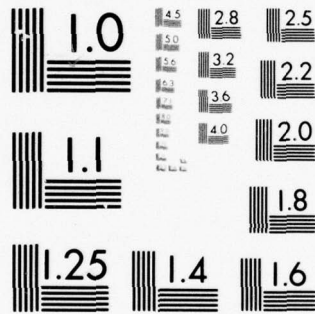
| OF |

AD  
A038873



END

DATE  
FILMED  
5-77



MICROCOPY RESOLUTION TEST CHART  
NATIONAL BUREAU OF STANDARDS-1963-A

364102

# 1832

*(Handwritten signature)*

ADA 038873

HYDRODYNAMICS OF CYLINDERS IN WATER OF  
ARBITRARILY VARYING DEPTH

By Yoon-Ho Kim

MASSACHUSETTS INSTITUTE OF TECHNOLOGY

May 1976

DDC  
RECEIVED  
APR 29 1977  
RESOLVED

*(Handwritten initials)* B

APPROVED FOR PUBLIC RELEASE:  
DISTRIBUTION UNLIMITED

AD No. \_\_\_\_\_  
DDC FILE COPY

UNCLASSIFIED

SECURITY CLASSIFICATION OF THIS PAGE (When Data Entered)

REPORT DOCUMENTATION PAGE		READ INSTRUCTIONS BEFORE COMPLETING FORM
1. REPORT NUMBER	2. GOVT ACCESSION NO.	3. RECIPIENT'S CATALOG NUMBER (9) Master's thesis
4. TITLE (and Subtitle) HYDRODYNAMICS OF CYLINDERS IN WATER OF ARBITRARILY VARYING DEPTH.		5. TYPE OF REPORT & PERIOD COVERED M.S. Thesis
		6. PERFORMING ORG. REPORT NUMBER
7. AUTHOR(s) Yoon-Ho Kim	8. CONTRACT OR GRANT NUMBER(s) N00014-75-C-0236 NSF-GK-43886X	
9. PERFORMING ORGANIZATION NAME AND ADDRESS Department of Ocean Engineering Massachusetts Institute of Technology Cambridge, Mass 02139		10. PROGRAM ELEMENT, PROJECT, TASK AREA & WORK UNIT NUMBERS SR 230101 Task 19077 PE
11. CONTROLLING OFFICE NAME AND ADDRESS David W. Taylor Naval Ship Research and Develop- ment Center, (1505), Bethesda, Md 20084		12. REPORT DATE 11 May 76
		13. NUMBER OF PAGES 67 (1269p)
14. MONITORING AGENCY NAME & ADDRESS (if different from Controlling Office) Office of Naval Research 800 N. Quincy St Arlington, Va 22217		15. SECURITY CLASS. (of this report) UNCLASSIFIED
		15a. DECLASSIFICATION/DOWNGRADING SCHEDULE
16. DISTRIBUTION STATEMENT (of this Report) APPROVED FOR PUBLIC RELEASE: DISTRIBUTION UNLIMITED 16 SR02301 17 SR0230101		
17. DISTRIBUTION STATEMENT (of the abstract covered in Block 20, if different from Report)		
18. SUPPLEMENTARY NOTES Sponsored by the Naval Sea Systems Command General Hydro- mechanics Research Program administered by the David W. Taylor Naval Ship R&D Center, Code 1505, Bethesda, Md. 20084 Co-Sponsored by National Science Foundation		
19. KEY WORDS (Continue on reverse side if necessary and identify by block number) Free-Surface Hydrodynamics, Numerical Technique, Waves, Fluid Motion Ocean Engineering		
20. ABSTRACT (Continue on reverse side if necessary and identify by block number) A numerical method for solving two-dimensional boundary-value problems related to time-harmonic potential flows with a free-surface is introduced. There is no restrictions on the body geometry nor the bottom topography. The entire fluid domain is subdivided into two regions, an inner region where all the geometrical changes occur and an outer region where the fluid depths are constant. Application of Green's theorem for an inner region results in an integral relation while the outer region is described by eigenfunction ex- pansions. A continuity of pressure and normal velocity across junction → next page		

UNCLASSIFIED

SECURITY CLASSIFICATION OF THIS PAGE (When Data Entered)

boundary imposes a unique solution in the entire fluid domain. The method is applied to both radiation and scattering problems and test results in water of finite or infinite depth agree well with the existing results.

UNCLASSIFIED

HYDRODYNAMICS OF CYLINDERS  
IN WATER OF ARBITRARILY VARYING DEPTH

by

Yoon-Ho Kim

B.S., Seoul National University  
(1971)

Submitted in Partial Fulfillment  
of the Requirement of the  
Degree of Master of  
Science

in  
Naval Architecture and  
Marine Engineering

at the  
MASSACHUSETTS INSTITUTE OF  
TECHNOLOGY

May 1976

REVISION for		
HTIS	White Section	<input checked="" type="checkbox"/>
DDC	Buff Section	<input type="checkbox"/>
UNANNOUNCED		<input type="checkbox"/>
JUSTIFICATION.....		
BY.....		
DISTRIBUTION/AVAILABILITY CODES		
Dist.	ATAIL	and/or SPECIAL
A		

Signature of Author..... *Yoon Ho Kim* .....  
Department of Ocean Engineering, 7 May 1976

Certified by..... *Ronald W. Young* .....  
Thesis Supervisor

Accepted by..... *J. H. Evans* .....  
Chairman, Departmental Committee on Graduate Students

HYDRODYNAMICS OF CYLINDERS  
IN WATER OF ARBITRARILY VARYING DEPTH

by

Yoon-Ho Kim

Submitted to the Department of Ocean Engineering on May 7, 1976 in partial fulfillment of the requirements for the degree of Master of Science in Naval Architecture and Marine Engineering.

ABSTRACT

A numerical method for solving two-dimensional boundary-value problems related to time-harmonic potential flows with a free-surface is introduced in this paper. There is no restrictions on the body geometry nor the bottom topography. The entire fluid domain is subdivided into two regions, an inner region where all the geometrical changes occur and an outer region where the fluid depths are constant. Application of Green's theorem for an inner region results in an integral relation while the outer region is described by eigenfunction expansions. A continuity of pressure and normal velocity across junction boundary imposes a unique solution in the entire fluid domain. The method is applied to both radiation and scattering problems and test results in water of finite or infinite depth agree well with the existing results.

Thesis Supervisor: Ronald W. Yeung  
Title: Assistant Professor of Ocean Engineering

#### ACKNOWLEDGEMENT

I would like to express my sincere gratitude to Professor Ronald W. Yeung for his encouragement and guidance during the course of this work.

I am also grateful to Dr. Kwang J. Bai and Dr. K.Y. Choo not only for their numerous suggestions on this study but also for their continuous advice throughout my stay at M.I.T.

Thanks are also due to my wife for her endless encouragement and assistance.

This work was supported by the Office of Naval Ship systems Command General Hydrodynamics Research Program administered by the Naval Ship Research and Development Center, Contract No. N00014-75-C-0236. Partial support by the National Science Foundation Grant GK-43886X is also acknowledged.

TABLE OF CONTENTS

	<u>page</u>
Title Page.....	1
Abstract.....	2
Acknowledgement.....	3
Table of Contents.....	4
List of Tables.....	6
List of Figures.....	7
I. INTRODUCTION.....	8
II. FORMULATION OF THE PROBLEM.....	12
II.1 Governing Equations and Boundary Conditions..	13
II.2 Pressure, Force, Moment and Free-Surface Elevation.....	14
III. SOLUTION OF THE PROBLEM.....	17
III.1 Application of Green's Theorem.....	18
III.2 Eigenfunction Expansions.....	20
III.3 Discretization of Integral Equation.....	25
IV. SCATTERING PROBLEMS.....	34
IV.1 Treatment of the Problem.....	34
IV.2 Relation Between Radiation and Scattering Problem.....	38
V. RESULTS AND DISCUSSION.....	40
V.1 Radiation Problem.....	40
i. Circular Cylinder in Heave and Sway.....	40
ii. Rectangular Cylinder in Heave and Sway.....	45
iii. Bulbous Section in Heave and Sway.....	45
V.2 Scattering Problem.....	50
i. Sinusoidal Hump.....	50
ii. Finite-Size Step.....	50
iii. Steep Hump at a Step.....	54

	<u>page</u>
VI. REMARKS.....	56
REFERENCES.....	57
APPENDICES.....	59
A. The Integrals $F_k$ and $G_k$ .....	59
B. Symmetry Relations for Radiation and Scattering Problems.....	63

LIST OF TABLES

	<u>page</u>
Table 1. Added-Mass, Damping Coefficients and Wave-Amplitude Ratio for Sway Motion.....	41
Table 2. Summary of Results for Varying the Location of Junction Boundary or the Number of Eigenfunctions.....	44
Table 3. Reflection and Transmission Coefficients of a Step.....	52
Table 4. Comparison of Reflection and Transmission Coefficients for Incident Waves in Opposite Directions.....	53

LIST OF FIGURES

	<u>page</u>
Fig. 1	Coordinate System and Cylinder in Oscillation. 17
Fig. 2	Subdivision of Contour..... 25
Fig. 3	Added-Mass and Amplitude Ratio for Circular Cylinder in Heave..... 43
Fig. 4	Added-Mass and Amplitude Ratio for Rectangular Cylinder in Heave..... 46
Fig. 5	Bottom Geometry with Bulbous Section..... 47
Fig. 6	a. Added-Mass and Damping Coefficients for Bulbous Section in Sway..... 48
	b. Hydrodynamic Coefficients for Bulbous Section in Heave..... 49
Fig. 7	Scattering Wave over Sinusoidal Hump..... 51
Fig. 8	Reflection and Transmission Coefficients of a Hump..... 55

## I. INTRODUCTION

Hydrodynamic research of two-dimensional bodies harmonically oscillating in or below the free surface of an ideal fluid has increased in importance in past decades and has been studied by a number of researchers. The 'radiation' problem applies to situation when waves are generated by forced oscillatory motion of the body in an otherwise undisturbed water. The modern history of this subject began with Ursell(1949), who formulated and solved the boundary-value problem for a semi-immersed heaving circular cylinder using linearized free-surface theory. He represented the velocity potential as the sum of an infinite set of multipoles, each satisfying the linear free-surface condition and each being multiplied by a coefficient determined by requiring the series to satisfy the kinematic boundary condition at a number of points on the cylinder. Grim(1953) used a variation of the Ursell method to solve the problem for two-parameter Lewis-form cylinders by conformal mapping onto circle. Tasai(1959) and Porter(1960), using the Ursell approach, obtained the added mass and damping for oscillating contours mappable onto a circle by the more general Theodorsen transformation. Ogilvie(1963) calculated the hydrodynamic forces on completely submerged circular cylinder. Lebreton

and Margnac(1966), Frank(1967) distributed the so-called wave-sources on the body contour and obtained the strength of these sources by solving a Fredholm integral equation of the second kind. This approach is still applicable when the depth is not constant, in which case the unknown strength in the integral equation will include also contribution from the bottom boundary.

The 'scattering' problem customarily refers to the interaction between incident plane waves and a fixed body. Various approaches have been used to tackle these problems associated with simple geometries. Newman(1965) provided results for the reflection and transmission coefficients over an infinite step by matching wave-maker solutions. Miles(1967) showed a more exact solution of the unequal-depths problem by using Schwinger's variational formulation. Hilaly(1967) treated the same problem by matching eigenfunction expansions. A more elegant approach, based upon a single source solution valid everywhere, may be constructed from the Green function derived by Evans(1971). Recently, Bai(1972) and Yeung(1973) investigated two new approaches for treating the problems of general bottom topography. The former utilized a variational formulation with the fluid domain represented by finite elements. The latter approach, on the other hand, consisted of applying a simple source function to the fluid domain, resulting in an integral

equation along the domain boundary that has to be solved.

While from the physical viewpoint, the scattering and radiation problems appear to be unrelated, from the mathematical viewpoint they differ only in terms of the boundary condition on the body and the far-field conditions. Many useful relations between them can be obtained as a result of application of Green's Theorem or a consequence of reciprocity principle.

The method investigated in this thesis stems from Yeung (1973) and Bai and Yeung (1974). The essence of the present approach lies in the exploitation of more than a single term in an eigenfunction expansions as previously used by Yeung (1973). This will have the net effect of shortening the boundary of the fluid, hence leads to an increase in computational efficiency. The overall approach to the solution of the two-dimensional radiation or scattering problems may be summarized as follows. The entire fluid domain is subdivided into two regions, an inner region where all the geometrical changes occur and an outer region(s) where the fluid depth is a constant. For the inner region, application of Green's second identity to the unknown velocity potential,  $\Phi(p)$  and the simple source function  $\log(1/r)$  give us an integral relation between  $\Phi(p)$  and its boundary values. For the outer region, the velocity potential is written in the form of an eigenfunction expansion with unknown complex

coefficients. At the junction boundaries where the inner and outer regions meet, a matching of the velocity potential and normal velocities is performed. This implies physically a continuity of pressure and flux across the artificial junction or "radiation" boundary. Such a matching process determines the solution uniquely in the entire fluid domain. We found that this method not only gives very accurate results compared with known values but also reduces computational time remarkably.

## II. FORMULATION OF THE PROBLEM

Consider the two-dimensional time-harmonic motion of an ideal fluid with a free-surface, as shown in Figure 1 on page 17. A right-handed rectangular coordinate system is used. The x-axis coincides with the undisturbed free-surface, the positive y-axis is taken upwards. The depth of fluid can be either finite or infinite. In the finite case, the bottom topography can be arbitrary, but must approach asymptotically constant depths  $h^+$  and  $h^-$ , which need not be equal. In order to use linearized water-wave theory, the following assumptions are required:

- a). the fluid is inviscid and incompressible;
- b). the effects of surface tensions are negligible;
- c). the fluid flow is irrotational;
- d). the fluid motion amplitudes and velocities are small enough that all but linear terms of the free-surface condition and the Bernoulli equation are neglected. The body boundary condition can be satisfied at an "mean" position, if the oscillations performed by the body are assumed small. Under the following assumptions, there exist a time-harmonic velocity potential which describes the motion of fluid.

## II.1 Governing Equations and Boundary Conditions

Let  $\Phi(x, y, t)$  be the velocity potential describing the flow field. The continuity equation requires  $\Phi$  to satisfy Laplace equation. Let  $\sigma$  be the angular frequency of the time-harmonic solution, then we have:

$$\Phi(x, y, t) = \text{Re} \{ \varphi(x, y) \dot{a}(t) \} \quad (2.1)$$

where  $\varphi = \varphi_1 + i\varphi_2$  is the unknown complex-valued spatial function, and  $a(t)$ , the complex time-harmonic amplitude of body, i.e.

$$\alpha(t) = \text{Re} [a(t)] \equiv \text{Re} [(a_1 + ia_2) e^{-i\sigma t}], \quad \dot{a} = \sqrt{-1} \quad (2.2)$$

where  $\alpha(t)$  is the body motion amplitude.

The unknown complex-valued spatial function,  $\varphi(x, y)$ , must satisfy Laplace equation throughout the fluid domain;

$$\nabla^2 \varphi(x, y) = 0 \quad (2.3a)$$

where  $\nabla^2 = \frac{\partial^2}{\partial x^2} + \frac{\partial^2}{\partial y^2}$

$$\vec{u}(x, y) = \frac{\partial \varphi}{\partial x}$$

$$\vec{v}(x, y) = \frac{\partial \varphi}{\partial y}$$

and also the following linearized boundary conditions;

$$\varphi_y - \nu \varphi = 0 \quad \text{on } S_F \quad (2.3b)$$

$$\frac{\partial \varphi}{\partial n} = \varphi_n = 0 \quad \text{on } S_B \quad (2.3c)$$

$$\varphi_n = V_n = f(s) \quad \text{on } S_0 \quad (2.3d)$$

where  $\nu = \frac{\sigma^2}{g}$ ,  $g$  being the acceleration of gravity.

Here,  $S_F$  is the undisturbed free surface,  $S_B$  the bottom surface, and  $S_O$  the wetted surface of the body at its equilibrium position. The normal vector  $\vec{n}$  is taken to be positive when pointing out of the fluid domain with components  $(n_x, n_y)$ . The only non-homogeneous boundary condition is (2.3d), which is given by  $f(s) = n_x, n_y$ , and  $(xn_y - yn_x)$ , each corresponding to the sway, heave and roll motion of the body respectively. The radiation condition, which states that the disturbance sufficiently far from the generating points must be outgoing waves, will render the solution unique.

## II.2 Pressure, Force, Moment and Free-Surface Elevation

The linearized hydrodynamic forces and moments acting on the body are given by;

$$\vec{F} = \int_{S_O} p \vec{n} \, ds \quad (2.4a)$$

$$\vec{M} = \int_{S_O} p (\vec{r} \times \vec{n}) \, ds \quad (2.4b)$$

where  $ds$  is the infinitesimal arc-length element and  $p$  can be obtained from the time-dependent Bernoulli equation,

$$p(x, y, t) = -\rho \Phi_t - \rho g y \quad (2.4c)$$

where  $\rho$  denoting the density of fluid. The first term in (2.4c) corresponds to the hydrodynamic pressure which is our primary concern and the second the hydrostatic pressure.

If we make use of (2.2) in (2.4c), (2.4a) and (2.4b) then yield,

$$F_j = - \int_{S_0} \rho \Phi_t n_j ds = - \rho \sum_{i=1}^3 \left[ \int_{S_0} \Phi_i^{(i)} n_j ds \right] \ddot{\alpha}_i(t) - \rho \sigma \sum_{i=1}^3 \left[ \int_{S_0} \Phi_2^{(i)} n_j ds \right] \dot{\alpha}_i(t), \quad j=1,2 \quad (2.5a)$$

$$M_j = - \int_{S_0} \rho \Phi_t (\vec{r} \times \vec{n})_j ds = - \rho \sum_{i=1}^3 \left[ \int_{S_0} \Phi_i^{(i)} n_j ds \right] \ddot{\alpha}_i - \rho \sigma \sum_{i=1}^3 \left[ \int_{S_0} \Phi_2^{(i)} n_j ds \right] \dot{\alpha}_i, \quad j=3 \quad (2.5b)$$

where  $i=1,2,3$  correspond to the sway, heave and roll motion respectively. Let's introduce the notation  $F_3=M_3$  and define

$$N_{ji} + i \frac{1}{\sigma} \lambda_{ji} = \rho \int_{S_0} \Phi^{(i)} n_j ds, \quad i,j=1,2,3 \quad (2.6)$$

then the force (or moment) component in the  $j$ -th direction can be written as

$$F_j = - N_{ji} \ddot{\alpha}_i(t) - \lambda_{ji} \dot{\alpha}_i(t) \quad (2.7)$$

where repeated indices are summed from 1 to 3. The  $N_{ji}$  are called 'added mass' or 'moment of added mass', depending on their dimensions, and each represents the fluid reaction in the  $j$ -th direction due to an acceleration of the body in the  $i$ -th direction. The  $\lambda_{ji}$  are called 'damping coefficients' and correspond to fluid reactions in phase with velocities. The free-surface elevation  $\zeta(x,t)$  can be obtained from the dynamic boundary condition of the free-surface and can be written as

$$\xi(x, t) = \text{Re} [ Y(x) e^{-i\sigma t} ] \quad (2.8a)$$

where

$$Y(x) = \nu \varphi(x, 0) (a_1 + i a_2) \quad (2.8b)$$

Hence if the potential is known on the free surface, the free-surface elevation can be calculated easily.

### III. SOLUTION OF THE PROBLEM

One difficulty in the numerical solution of the radiation or forced-motion problem is that the radiation condition in principle should be applied as  $x = \pm \infty$ . In practice, the infinite boundaries have to be truncated at a finite range with appropriate reasonings, the result of such truncation implies local disturbances must be accounted for. The behavior of local disturbances can be examined by making use of the eigenfunction expansions.

First let  $\Sigma_+, \Sigma_-$  be two arbitrarily chosen vertical boundaries which subdivide the fluid domain into an inner region of arbitrary bottom and the body and two outer regions of horizontally uniform depths. Let these regions be designated I, II and III as shown in Figure 1.

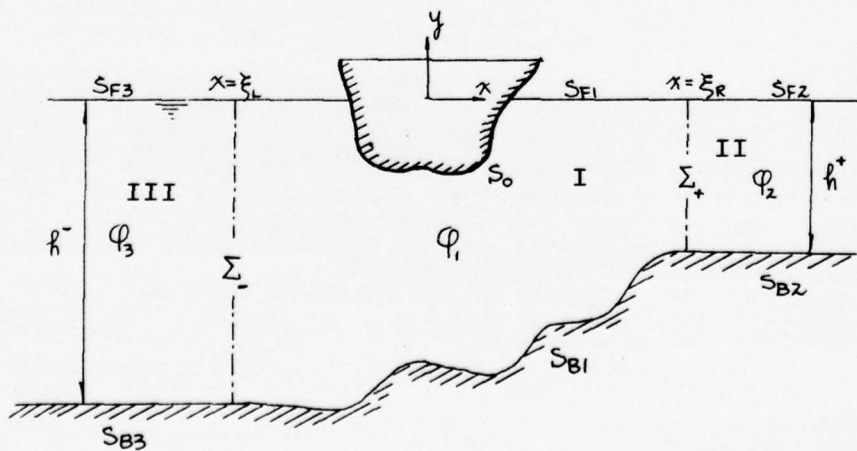


Fig.1 Coordinate System and Cylinder in Oscillation

Let  $\varphi_1, \varphi_2$  and  $\varphi_3$  denote the complex-valued potential functions in each region, then we have the boundary-value problems as follows:

$$\begin{aligned}
 \nabla^2 \varphi &= 0 && \text{in fluid domain (I, II, III)} \\
 \varphi_y - \nu \varphi &= 0 && \text{on } S_F \quad (\text{I, II, III}) \\
 \varphi_n = V_n = f(s) &&& \text{on } S_O \quad (\text{I}) \quad (3.1) \\
 \varphi_n &= 0 && \text{on } S_B \quad (\text{I, II, III}) \\
 \lim (\varphi_\alpha \mp i m_0 \varphi) &= 0, \quad \alpha \rightarrow \pm \infty && (\text{II, III})
 \end{aligned}$$

We need some additional conditions for matching the pressure and flux which are proportional to the velocity potential and normal velocity respectively, at the arbitrarily chosen boundaries;

$$\begin{aligned}
 \varphi_1 = \varphi_2, \quad \varphi_{1n} = -\varphi_{2n} & \quad \text{at } \Sigma_+ \\
 \varphi_1 = \varphi_3, \quad \varphi_{1n} = -\varphi_{3n} & \quad \text{at } \Sigma_-
 \end{aligned} \quad (3.2)$$

With these matching conditions, the complex-valued functions  $\varphi_1, \varphi_2$  and  $\varphi_3$  would be properly coupled together and represent a unique solution for the entire fluid domain.

### III.1 Application of Green's Theorem

Referring to Figure 1, we assume that  $\varphi$  is a smooth function whose first and second derivatives are continuous everywhere in the fluid domain. Application of Green's second identity to the unknown complex function  $\varphi_1$  and the

source function  $\log(1/r)$  in Region I, yields the following well-known theorem :

$$2\pi\varphi_1(P) = \oint_S \frac{\partial\varphi_1(Q)}{\partial n} \log\left(\frac{1}{r}\right) ds(Q) - \oint_S \varphi_1(Q) \frac{\partial}{\partial n} \log\left(\frac{1}{r}\right) ds(Q), \quad (3.3)$$

where  $P = (x,y)$  is a field point in Region I and  $Q = (\xi,\eta)$  is a variable point on the fluid boundary,  $S = S_{O\cup} S_{F1\cup} \Sigma_+ \cup S_{B1\cup} \Sigma_-$ . Here  $r$  is the distance between points  $P$  and  $Q$ ,  $ds(Q)$  an infinitesimal arc-length element along the fluid boundary  $S$ , and  $\frac{\partial}{\partial n} = \vec{n} \cdot \left(\frac{\partial}{\partial \xi}, \frac{\partial}{\partial \eta}\right)$ ,  $\xi, \eta$  being variables of integration along  $S$ .

From the boundary conditions (3.1), we observe that the normal derivatives of  $\varphi_1$  are either known or expressed in terms of  $\varphi_1$  itself on  $S$  except for  $\Sigma_+$  and  $\Sigma_-$ . Therefore (3.3) can be written as follows :

$$\begin{aligned} 2\pi\varphi_1(P) = & \int_{S_0} \varphi_1(Q) \frac{\partial}{\partial n} \log r ds(Q) + \int_{S_{F1}} \varphi_1 \left[ \frac{\partial}{\partial n} \log r - \nu \log r \right] ds \\ & + \int_{\Sigma_+} \left[ \varphi_1 \frac{\partial}{\partial n} \log r - \varphi_{1n} \log r \right] ds + \int_{S_{B1}} \varphi_1 \frac{\partial}{\partial n} \log r ds \\ & + \int_{\Sigma_-} \left[ \varphi_1 \frac{\partial}{\partial n} \log r - \varphi_{1n} \log r \right] ds - \int_{S_0} f(s) \log r ds \end{aligned} \quad (3.4)$$

Note that we have place no restrictions on the shape of body and geometry of bottom. This integral relation merely represents the distributions of simple source and normal dipoles with a certain amount of strength along the contour  $S$ .

### III.2 Eigenfunction Expansions

Now let us consider Regions II and III. The boundary of Region II consists of a free surface  $S_{F2}$ , the horizontal bottom  $S_{B2}$  and the "junction" boundary  $\Sigma_+$ . By using the method of separation of variables, one can obtain the fundamental solutions in the form of eigenfunction expansions easily. (Wehausen & Laitone, 1960)

These eigenfunctions are

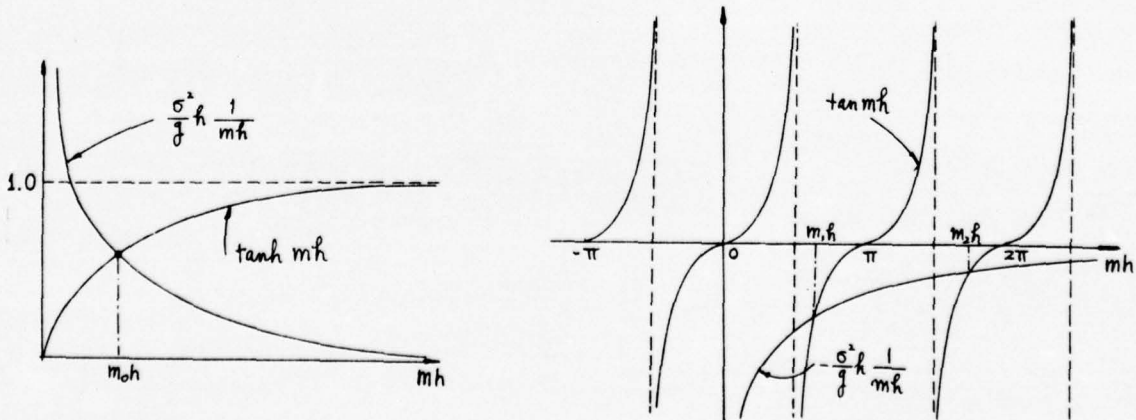
$$\left\{ \frac{\cosh m_0(h+y)}{\cosh m_0 h} e^{im_0 x}, \frac{\cos m_k(h+y)}{\cos m_k h} e^{-m_k x} \right\}$$

where the eigenvalues  $m_0, m_1, m_2, \dots, m_k, \dots$  are roots of the transcendental equations;

$$m_0 \tanh m_0 h = \frac{\sigma^2}{g} \quad (3.5)$$

$$m_k \tan m_k h = -\frac{\sigma^2}{g} \quad (k = 1, 2, 3, \dots)$$

Eigenvalues are shown graphically below :



The orthogonality of eigenfunctions can be easily verified by direct computation on the interval  $-h \leq y \leq 0$ . These are all the consequence of Sturm-Liouville theory (Hildebrand, 1948). With a similar representation in Region III, we may write the solutions as follows;

$$\varphi_2(x, y) = A_0^+ e^{im_0^+ x} \frac{\cosh m_0^+(y+h^+)}{\cosh m_0^+ h^+} + \sum_{k=1}^{\infty} C_k^+ e^{-m_k^+ x} \frac{\cos m_k^+(y+h^+)}{\cos m_k^+ h^+}$$

for Region II (3.6)

$$\varphi_3(x, y) = A_0^- e^{-im_0^- x} \frac{\cosh m_0^-(y+h^-)}{\cosh m_0^- h^-} + \sum_{k=1}^{\infty} C_k^- e^{m_k^- x} \frac{\cos m_k^-(y+h^-)}{\cos m_k^- h^-}$$

for Region III (3.7)

where the superscripts + and - denote Regions II and III respectively. The coefficients  $A_0$  and  $C_k$  are unknown complex values. Note that the first term of (3.6) or (3.7) corresponds to propagating waves, the second to purely local disturbance. Note also the functional forms of (3.6) and (3.7) are chosen so that  $\varphi_2$  and  $\varphi_3$  represent outgoing waves propagating to the right and left respectively. It is clearly not practical to take an infinite number of terms in (3.6) and (3.7). To assist us in deciding the number of terms to be taken in the series, let us define the decay factor from (3.6) or (3.7) by

$$\delta(k, x) = e^{\mp m_k x} \quad \text{for } x \geq 0$$

Assuming  $C_k = O(1)$ , and that  $\varepsilon$  is a tolerance parameter, say,  $10^{-6}$ , we may choose  $N^{R,L}$ , the number of terms to be taken in the series, either by finding  $N^{R,L}$  such that  $\delta(N^R, \xi_R) < \varepsilon$  and  $\delta(N^L, \xi_L) < \varepsilon$  for a given  $\xi_R$  and  $\xi_L$ , or finding  $\xi_R$  and  $\xi_L$  satisfying the same criteria for given  $N^{R,L}$ . This serves somewhat as a guide only, because in actuality  $C_k$  could be quite large. However convergence of the series is guaranteed by the fact that  $C_k e^{-m_k x}$  remain small.

Now we are in a position to apply the matching condition (3.2) at the junction boundaries  $\Sigma_+$ ,  $\Sigma_-$ . If we make use of  $\varphi_2$  and  $\varphi_3$  and substitute them into  $\varphi_1$  at  $\Sigma_+$  and  $\Sigma_-$ , we may rewrite (3.4) as :

$$\begin{aligned}
 2\pi\varphi_1(P) = & \int_{S_0} \varphi_1(Q) \frac{\partial}{\partial n} \log r \, ds(Q) + \int_{S_{F1}} \varphi_1 \left( \frac{\partial}{\partial n} \log r - \nu \log r \right) ds \\
 & + \int_{S_B} \varphi_1 \frac{\partial}{\partial n} \log r \, ds - \int_{S_0} f(s) \log r \, ds \\
 & + A_0^+ e^{-im_0^+ \xi_R} (\mathcal{F}_0^+ - iG_0^+) + \sum_{k=1}^{N^R} C_k^+ e^{-m_k^+ \xi_R} (\mathcal{F}_k^+ + G_k^+) \\
 & - A_0^- e^{-im_0^- \xi_L} (\mathcal{F}_0^- + iG_0^-) + \sum_{k=1}^{N^L} C_k^- e^{m_k^- \xi_L} (\mathcal{F}_k^- + G_k^-) \quad (3.8)
 \end{aligned}$$

where the functions  $\mathcal{F}_k(x-\xi, y)$  and  $G_k(x-\xi, y)$  are defined by the following integrals ;

$$\begin{aligned}
 \mathcal{F}_0(x-\xi, y) &= \int_{-h}^0 d\eta \frac{\cosh m_0(\eta+h)}{\cosh m_0 h} \left\{ \frac{\partial}{\partial \xi} \log r \right\} \\
 G_0(x-\xi, y) &= \int_{-h}^0 d\eta \frac{\cosh m_0(\eta+h)}{\cosh m_0 h} \left\{ m_0 \log r \right\}
 \end{aligned} \quad (3.9)$$

$$\begin{aligned} \mathcal{F}_k(x-\xi, y) &= \int_{-h}^0 d\eta \frac{\cos m_k(\eta+h)}{\cos m_k h} \left\{ \begin{array}{l} \frac{\partial}{\partial \xi} \log r \\ m_k \log r \end{array} \right\}, \quad k=1, 2, \dots \quad (3.10) \\ \mathcal{G}_k(x-\xi, y) & \end{aligned}$$

From now on, subscript '1' will be dropped with the understanding that we seek only  $\varphi$  in Region I.

One can easily recognize that the last four terms of (3.8) represent vertical distributions of simple sources and normal dipoles with the functional forms of the strength being the same as the eigenfunction in the vertical direction. Referring to (3.8) we see that the spatial velocity potential  $\varphi(P)$  will be known everywhere if  $\varphi(Q)$  is determined on the boundaries  $S_{OV}, S_{BV}, S_F$ , and if the coefficients of the eigenfunctions are determined. To obtain an equation for the  $\varphi(Q)$ , we let the field point  $P$  approach the fluid boundary  $S$ . The following integral equation then results :

$$\begin{aligned} & -\pi\varphi(P) + \int_{S_{OV}S_B} \varphi \frac{\partial}{\partial n} \log r \, ds + \int_{S_F} \varphi \left( \frac{\partial}{\partial n} \log r - \nu \log r \right) ds \\ & + A_0^+ e^{im_0^+ \xi_R} (\mathcal{F}_0^+ - i\mathcal{G}_0^+) + \sum_{k=1}^{N_R} C_k^+ e^{-m_k^+ \xi_R} (\mathcal{F}_k^+ + \mathcal{G}_k^+) \\ & - A_0^- e^{-im_0^- \xi_L} (\mathcal{F}_0^- + i\mathcal{G}_0^-) + \sum_{k=1}^{N_L} C_k^- e^{m_k^- \xi_L} (\mathcal{F}_k^- + \mathcal{G}_k^-) \\ & = \int_{S_0} f(s) \log r \, ds \end{aligned}$$

for  $P \in S$ . (3.11)

Note that to determine the unknown complex coefficients of eigenfunction, we need  $(N_R+1)$  distinct locations on  $\Sigma_+$  and  $(N_L+1)$  distinct locations on  $\Sigma_-$  when the field point P is placed at each junction boundary. In this case  $\Phi(P)$  can be expressed as the eigenfunction expansions themselves, i.e.,

$$\begin{aligned} & \int_{S_{0V} S_B} \Phi\left(\frac{\partial}{\partial n} \log r\right) ds + \int_{S_F} \Phi\left(\frac{\partial}{\partial n} \log r - \nu \log r\right) ds \\ & + A_0^+ e^{im_0^+ \xi_R} \left[ -\pi \frac{\cosh m_0^+(y+h^+)}{\cosh m_0^+ h^+} - i G_0^+(0, y) \right] + \sum_{k=1}^{N_R} C_k^+ e^{-m_k^+ \xi_R} \\ & \left[ -\pi \frac{\cos m_k^+(y+h^+)}{\cos m_k^+ h^+} + G_{T_k}^+(0, y) \right] - A_0^- e^{-im_0^- \xi_L} \left[ J_0^-(\xi_R - \xi_L, y) + i G_0^-(\xi_R - \xi_L, y) \right] \\ & + \sum_{k=1}^{N_L} C_k^- e^{m_k^- \xi_L} \left[ J_k^-(\xi_R - \xi_L, y) + G_{T_k}^-(\xi_R - \xi_L, y) \right] = \int_{S_0} f(s) \log r ds \\ & \text{for } P \in \Sigma_+ \quad (3.12) \end{aligned}$$

and

$$\begin{aligned} & \int_{S_{0V} S_B} \Phi\left(\frac{\partial}{\partial n} \log r\right) ds + \int_{S_F} \Phi\left(\frac{\partial}{\partial n} \log r - \nu \log r\right) ds \\ & + A_0^+ e^{im_0^+ \xi_R} \left[ J_0^+(\xi_L - \xi_R, y) - i G_0^+(\xi_L - \xi_R, y) \right] + \sum_{k=1}^{N_R} C_k^+ e^{m_k^+ \xi_R} \left[ J_k^+(\xi_L - \xi_R, y) + G_{T_k}^+(\xi_L - \xi_R, y) \right] \\ & - A_0^- e^{-im_0^- \xi_L} \left[ \pi \frac{\cosh m_0^-(y+h^-)}{\cosh m_0^- h^-} + i G_0^-(0, y) \right] + \sum_{k=1}^{N_L} C_k^- e^{m_k^- \xi_L} \\ & \left[ -\pi \frac{\cos m_k^-(y+h^-)}{\cos m_k^- h^-} + G_{T_k}^-(0, y) \right] = \int_{S_0} f(s) \log r ds \\ & \text{for } P \in \Sigma_- \quad (3.13) \end{aligned}$$

It is worthwhile to remark that the choice of  $P$  on  $\Sigma_+$  and  $\Sigma_-$  has little effect on the numerical solution of the problem. This was verified by a sequence of numerical experiments. Of course, one must not choose two points to be so close that they become numerically indistinctive.

### III.3 Discretization of Integral Equation

The method of discretization will be used to obtain an approximate solution of the integral equation (3.11) for the unknown function  $\varphi(Q)$ . Such method reduces the integral equation to a set of linear algebraic equations. We followed the scheme used by Yeung (1973). Referring to Figure 2

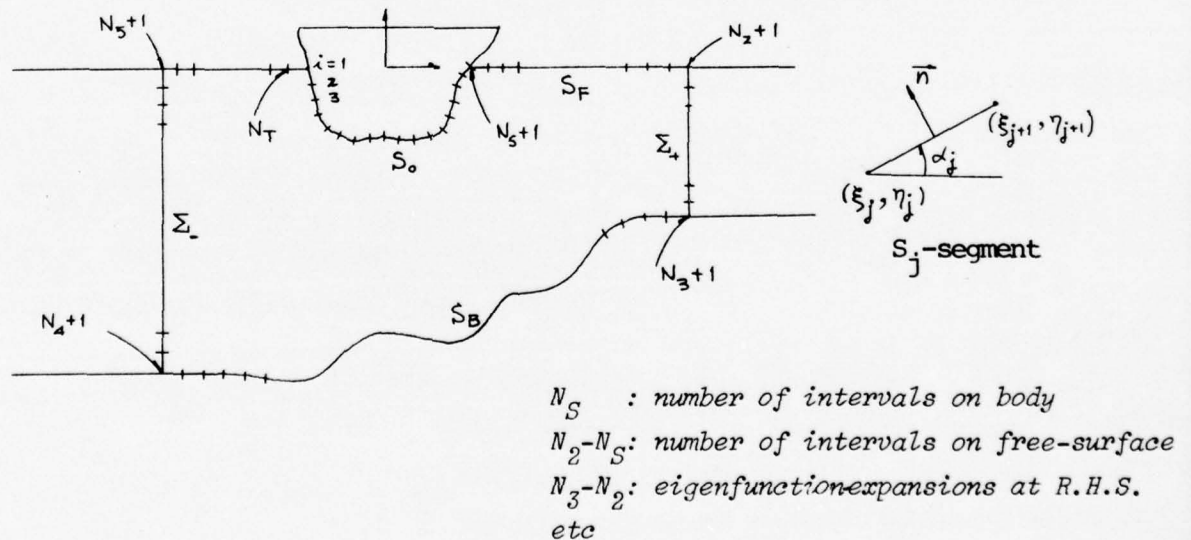


Fig. 2 Subdivision of Contour

the contour  $S_O, S_F$  and  $S_B$  in Region I is first subdivided into a number of small segments. Then each segment can be considered as a straight line joining a pair of grid points  $(\xi_j, \eta_j), (\xi_{j+1}, \eta_{j+1})$ .

For a sufficiently fine division, the unknown  $\varphi(Q)$  between a pair of grid points may be approximated by some distribution function. In present case  $\varphi(Q)$  is assumed to be a constant function and represented by  $\varphi_j = \varphi\left(\frac{\xi_j + \xi_{j+1}}{2}, \frac{\eta_j + \eta_{j+1}}{2}\right)$ . As an illustration, let us consider the body contour integral along  $S_O$  ;

$$\begin{aligned} & \int_{S_O} \varphi \frac{\partial}{\partial n} \log \left[ (x-\xi)^2 + (y-\eta)^2 \right]^{\frac{1}{2}} ds \\ &= \sum_{j=1}^{N_S} \int_{S_j} \varphi \frac{\partial}{\partial n} \log r ds \end{aligned}$$

where  $S_O$  is broken up into a number of small segments  $S_j$ . in each segment,  $\varphi(s)$  may be approximated by constant. Hence it can be written as follows ;

$$\int_{S_O} \varphi \frac{\partial}{\partial n} \log \left[ (x-\xi)^2 + (y-\eta)^2 \right]^{\frac{1}{2}} ds \cong \sum_{j=1}^{N_S} \varphi_j Q_{ij}$$

with

$$Q_{ij} = \int_{(\xi_j, \eta_j)}^{(\xi_{j+1}, \eta_{j+1})} \frac{\partial}{\partial n_j} \log \left[ (x_i - \xi)^2 + (y_i - \eta)^2 \right]^{\frac{1}{2}} ds.$$

Similar operations on other parts of the contour then yield the following discretized representation of integral of (3.11)

$$\begin{aligned}
& -\pi \varphi(x_i, y_i) + \sum_{j=1}^{N_S} \varphi_j Q_{ij} + \sum_{j=N_S+1}^{N_2} \varphi_j (Q_{ij} - \nu P_{ij}) + A_0^+ S_0^+ \\
& + \sum_{k=1}^{N_R} C_k^+ S_{ik}^+ + \sum_{j=N_3+1}^{N_4} \varphi_j Q_{ij} + A_0^- S_{ik}^- + \sum_{k=1}^{N_L} C_k^- S_{ik}^- + \sum_{j=N_5+1}^{N_T} \varphi_j (Q_{ij} - \nu P_{ij}) \\
& = \sum_{j=1}^{N_S} f(x_j, y_j) P_{ij}, \quad \begin{aligned} & i=1, 2, \dots, N_S, N_S+1, \dots, N_2 \\ & i=N_3+1, \dots, N_4, \quad (3.14) \\ & i=N_5+1, \dots, N_5, \end{aligned}
\end{aligned}$$

where  $(x_i, y_i)$  denotes the control or observation point and

$$P_{ij} = \int_{(\xi_j, \eta_j)}^{(\xi_{j+1}, \eta_{j+1})} \frac{1}{2} \log \left[ (x_i - \xi)^2 + (y_i - \eta)^2 \right] ds \quad (3.15)$$

$$Q_{ij} = \int_{(\xi_j, \eta_j)}^{(\xi_{j+1}, \eta_{j+1})} \frac{\partial}{\partial n_j} \log \left[ (x_i - \xi)^2 + (y_i - \eta)^2 \right]^{\frac{1}{2}} ds$$

and

$$S_{i0}^{\pm} = e^{\pm i m_0^{\pm} \xi} \left[ \pm \mathcal{F}_0^{\pm}(x_i - \xi, y_i) - i \mathcal{G}_0^{\pm}(x_i - \xi, y_i) \right] \quad (3.16a)$$

$$S_{ik}^{\pm} = \left[ \pm \mathcal{F}_k^{\pm}(x_i - \xi, y_i) - i \mathcal{G}_k^{\pm}(x_i - \xi, y_i) \right], \quad k=1, 2, \dots \quad (3.16b)$$

with  $\mathcal{F}_k$  and  $\mathcal{G}_k$  defined by (3.9) and (3.10), and +, - denoting right and left junction or "radiation" boundary respectively. Using a more compact notation, equation (3.14) can be rewritten as follow :

$$\sum_j (-\pi \delta_{ij} + C_{ij}) \Phi_j + A_0^+ S_{i0}^+ + \sum_{k=1}^{NR} C_k^+ S_{ik}^+ + A_0^- S_{i0}^- + \sum_{k=1}^{NR} C_k^- S_{ik}^- = \sum_{j=1}^{N_5} f(x_j, y_j) P_{ij} \quad i=1, 2, \dots, N_T \quad (3.17)$$

where  $\delta_{ij}$  is the Kronecker delta and the coefficient  $C_{ij}$  are defined as follows

$$C_{ij} = \begin{cases} Q_{ij} & \text{for } j=1, \dots, N_5; N_3+1, \dots, N_4; \\ Q_{ij} - \nu P_{ij} & \text{for } j=N_5+1, \dots, N_2; N_5+1, \dots, N_T \end{cases} \quad (3.18)$$

When we place the control points on junction boundary  $\Sigma_+$ , (3.17) needs a slight modification for (3.12) should be used instead of (3.11). In this case, the unknown velocity potential can be represented by eigenfunction itself, namely,

$$\Phi(P) = A_0^+ \frac{\cosh m_0^+(y+l^+)}{\cosh m_0^+ l^+} e^{-i m_0^+ \xi_R} + \sum_{k=1}^{NR} C_k^+ \frac{\cos m_k^+(y+l^+)}{\cos m_k^+ l^+} e^{-m_k^+ \xi_R} \quad \text{for } P = (\xi_R, y) \quad (3.19)$$

If we make use of (3.19) in (3.12), the following equation then results:

$$\sum_{j=1}^{N_5} \Phi_j Q_{ij} + \sum_{j=N_5+1}^{N_2} \Phi_j (Q_{ij} - \nu P_{ij}) + A_0^+ T_{i0}^+ + \sum_{k=1}^{NR} C_k^+ T_{ik}^+ + \sum_{j=N_5+1}^{N_4} \Phi_j Q_{ij} + A_0^- S_{i0}^- + \sum_{k=1}^{NR} C_k^- S_{ik}^- = \sum_{j=1}^{N_5} P_{ij} f(x_j, y_j) \quad \text{for } i=N_2+1, \dots, N_3 \quad (3.20)$$

where  $T_{ik}^+$  are defined by

$$T_{i0}^+ = e^{im_0^+ \xi_R} \left[ -\pi \frac{\cosh m_0^+(y+h^+)}{\cosh m_0^+ h^+} + i G_0^+(0, y) \right]$$

$$T_{ik}^+ = -\pi \frac{\cos m_k^+(y+h^+)}{\cos m_k^+ h^+} + G_{TK}^+(0, y)$$
(3.21)

If the control points are placed on  $\Sigma_-$ , the velocity potential can be written as ;

$$\Phi(P) = A_0^- \frac{\cosh m_0^-(y+h^-)}{\cosh m_0^- h^-} e^{-im_0^- \xi_L} + \sum_{k=1}^{N_L} C_k^- \frac{\cos m_k^-(y+h^-)}{\cos m_k^- h^-} e^{m_k^- \xi_L}$$

for  $P = (\xi_L, y)$  (3.22)

and the following results are obtained by making use of (3.22) in (3.13):

$$\sum_{j=1}^{N_S} \Phi_j Q_{ij} + \sum_{j=N_S+1}^{N_Z} \Phi_j (Q_{ij} - \nu P_{ij}) + A_0^+ S_{i0}^+ + \sum_{k=1}^{N_R} C_k^+ S_{ik}^+$$

$$+ \sum_{j=N_S+1}^{N_Z} Q_{ij} \Phi_j - A_0^- T_{i0}^- + \sum_{k=1}^{N_L} C_k^- T_{ik}^- = \sum_{j=1}^{N_S} P_{ij} f(x_j, y_j)$$
(3.23)

where

$$T_{i0}^- = e^{-im_0^- \xi_L} \left[ -\pi \frac{\cosh m_0^-(y+h^-)}{\cosh m_0^- h^-} + i G_0^-(0, y) \right]$$

$$T_{ik}^- = -\pi \frac{\cos m_k^-(y+h^-)}{\cos m_k^- h^-} + G_{TK}^-(0, y)$$
(3.24)

Now for Equation (3.14), (3.20) and (3.23), we have altogether  $N_T$  linear algebraic equations for  $N_T$  unknowns which can be solved simultaneously. The remaining problem we face now is the efficient evaluation of the integrals defined by in (3.9), (3.10) and (3.15). The  $P_{ij}$ 's and  $Q_{ij}$ 's can be evaluated analytically in a rather straight-forward manner:

$$\begin{aligned}
 P_{ij}(\xi_j, \eta_j; \xi_{j+1}, \eta_{j+1}) &= \int_{S_j} \log[(x_i - \xi)^2 + (y_i - \eta)^2]^{\frac{1}{2}} ds \\
 &= \cos \alpha_j \left\{ (\xi_j - \xi_{j+1}) - \frac{1}{2}(x_i - \xi_{j+1}) \cdot \log[(x_i - \xi_{j+1})^2 + (y_i - \eta_{j+1})^2] \right. \\
 &\quad \left. + \frac{1}{2}(x_i - \xi_j) \log[(x_i - \xi_j)^2 + (y_i - \eta_j)^2] \right\} + \sin \alpha_j \left\{ (\eta_j - \eta_{j+1}) \right. \\
 &\quad \left. - \frac{1}{2}(y_i - \eta_{j+1}) \log[(x_i - \xi_{j+1})^2 + (y_i - \eta_{j+1})^2] + \frac{1}{2}(y_i - \eta_j) \log[(x_i - \xi_j)^2 + (y_i - \eta_j)^2] \right\} \\
 &\quad - Q_{ij} \left\{ (y_i - \eta_{j+1}) \cos \alpha_j - (x_i - \xi_{j+1}) \sin \alpha_j \right\}
 \end{aligned} \tag{3.25a}$$

$$\begin{aligned}
 Q_{ij}(\xi_j, \eta_j; \xi_{j+1}, \eta_{j+1}) &= \int_{S_j} \frac{\partial}{\partial \eta_j} \log[(x_i - \xi)^2 + (y_i - \eta)^2]^{\frac{1}{2}} ds \\
 &= \tan^{-1} \left( \frac{y_i - \eta_j}{x_i - \xi_j} \right) - \tan^{-1} \left( \frac{y_i - \eta_{j+1}}{x_i - \xi_{j+1}} \right)
 \end{aligned} \tag{3.25b}$$

For  $F_k$  and  $G_k$  simple closed-form solutions appear not possible. While (3.16a) does not pose too much of a problem for numerical quadrature, (3.16b) have rapidly oscillatory integrands, especially when  $m_k$  becomes large. We found that

these source and normal-dipole integrals having oscillatory behavior can actually be written in terms of standard exponential integral with complex argument. To avoid disruption of the continuity of exposition of the main text, we provide all details of the derivation in Appendix A, which is based on a contour-interpretation of this integrals in the complex plane\*. The results can be summarized as follows.

Define the complex quantities:

$$\zeta_1 = m[(x-\xi) + iy], \quad \zeta_2 = m[(x-\xi) + i(y+h)], \quad y \leq 0 \quad (3.25)$$

then

$$\begin{aligned} \mathcal{F}_k(x-\xi, y) &= \int_{-h}^0 \cos m(\eta+h) \frac{\partial}{\partial \xi} \left\{ \log [(x-\xi)^2 + (y-\eta)^2]^{\frac{1}{2}} \right\} d\eta \\ &= -\pi \operatorname{sgn}(x-\xi) e^{-|x-\xi|m} \cos m(y+h) \\ &= \frac{1}{2} \int_m \left[ e^{\zeta_2} E_1(\zeta_2) + e^{-\zeta_2} E_1(-\zeta_2) - e^{i\zeta_1} e^{\zeta_1} E_1(\zeta_1) - e^{-i\zeta_1} e^{-\zeta_1} E_1(-\zeta_1) \right] \end{aligned} \quad (3.26)$$

$$\begin{aligned} \mathcal{G}_k(x-\xi, y) &= m \int_{-h}^0 \cos m(\eta+h) \log [(x-\xi)^2 + (y-\eta)^2]^{\frac{1}{2}} d\eta \\ &= \sin mh \log [(x-\xi)^2 + y^2]^{\frac{1}{2}} - \pi \cos m(h+y) e^{-|x-\xi|m} \\ &= -\frac{1}{2} \int_m \left[ e^{\zeta_2} E_1(\zeta_2) - e^{-\zeta_2} E_1(-\zeta_2) - e^{i\zeta_1} e^{\zeta_1} E_1(\zeta_1) + e^{-i\zeta_1} e^{-\zeta_1} E_1(-\zeta_1) \right] \end{aligned} \quad (3.27)$$

where the exponential integral function  $E_1(z)$  is defined

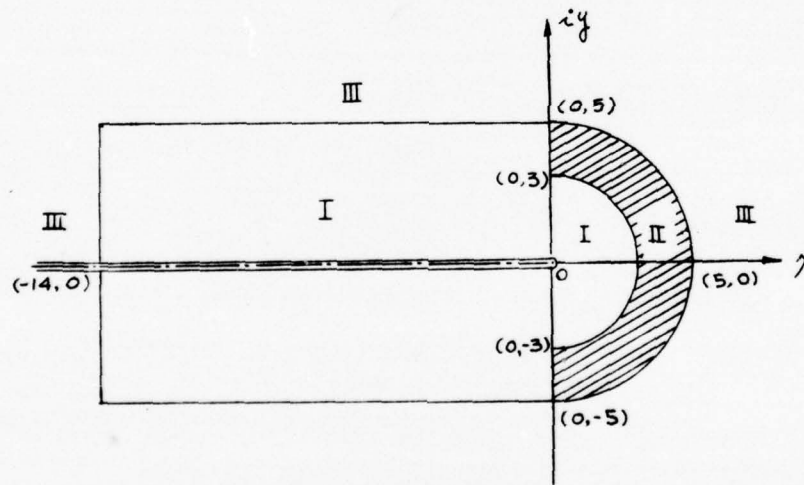
to be

\*The author is grateful to Prof. Yeung for providing him a copy of such derivation.

$$E_1(z) = \int_z^\infty \frac{e^{-t}}{t} dt, \quad |\arg z| < \pi.$$

(3.28)

We used two different methods of evaluating this exponential integral for complex arguments. One is the formal series expansions when the arguments are comparatively small and the second method is the use of Laguerre quadrature (Todd, 1954) for large arguments. The following graph shows in which range the two different methods are used separately.



In region I and II, we take the formal series expansions (Abramowitz & Stegun, 1970), i.e.,

$$E_1(z) = -\gamma - \ln z - \sum_{n=1}^{\infty} \frac{(-1)^n z^n}{n n!}, \quad |\arg z| < \pi$$

where  $\gamma (= .5772156649)$  is the Euler's constant and double-precision calculation is required in region II because of slow convergence. For region III, we introduce Laguerre quadrature method as follows:

$$e^{\gamma} E_1(\gamma) = I_1 - i I_2$$

where

$$I_1 = \int_0^{\infty} e^{-\rho} \frac{x+\rho}{(x+\rho)^2 + y^2} d\rho, \quad I_2 = \int_0^{\infty} e^{-\rho} \frac{y}{(x+\rho)^2 + y^2} d\rho$$

It is well known that, for any  $n$ ,

$$I = \int_0^{\infty} e^{-t} f(t) dt \cong \sum \lambda_i^{(n)} f(x_i^{(n)}) = Q$$

where the  $x_i^{(n)}$  are the zeros of the Laguerre polynomial  $L_n(t)$

and  $\lambda_i^{(n)}$  are the corresponding Christoffel numbers, or

weights. Moreover, it is known (Szegő, 1939) that for some  $\xi$ ,

the error

$$R = |I - Q| = (n!)^2 \frac{f^{(2n)}(\xi)}{2n!}$$

We can estimate  $R$  by

$$|R| \leq \frac{(n!)^2}{(x^2 + y^2)^{n+1/2}} \quad x \geq 0,$$

$$|R| \leq \frac{(n!)^2}{|y|^{2n+1}} \quad x < 0.$$

Hence one sees that difficulties in using the Laguerre

quadrature scheme are encountered when  $z$  approaches the

negative axis. To obtain a small value of  $|R|$ , we have

to make an optimum choice of  $n$ , which is about  $|z|$  in the

first case,  $|y|$  in the second. With this choice of  $n$ , we

find, using Stirling's formula, that the value of our bounds

for  $|R|$  are about  $2\pi e^{-2n}$  in each case.

## VI. SCATTERING PROBLEMS

### VI.1 Treatment Of The Problem

If we consider the scattering problem corresponding to an incoming wave system from the left with unit amplitude, the definition introduced in (2.1) for the complex function  $\Phi$  is still applicable provided one sets  $a_1=0$  and  $a_2=1/\sigma$ . The total velocity potential, known as the scattering potential, is normally decomposed into

$$\Phi_S = \Phi_I + \Phi_D \quad (4.1)$$

where  $\Phi_I$ , the incident wave spatial potential, is defined as:

$$\Phi_I = \frac{gA_I}{\sigma} \frac{\cosh m_0^-(y+h^-)}{\cosh m_0^-h^-} e^{im_0^-x} \quad (4.2)$$

$A_I$  being the incident wave amplitude, and  $\Phi_D$  is the so-called diffraction potential which usually has to be solved for. In our formulation, it is much more convenient to work with the scattering potential directly. The scattering potential (4.1) satisfies the boundary conditions (2.3b) and (2.3c), but for (2.3d)

$$(\Phi_S)_n = 0 \quad \text{on } S_0 \quad (4.3)$$

So far, we see that all boundary conditions for  $\Phi_S$  in Region I are homogeneous. The inhomogeneous boundary

condition clearly will come from the radiation boundary. To see this, we observe that equation (3.7) is no longer a complete representation of the solution in Region II. If the right-moving incident wave is of amplitude  $A_I$  in Region III, (3.7) should be replaced by

$$\Phi_S(x, y) = (A_I e^{im_0^- x} + A_0^- e^{-im_0^- x}) \frac{\cosh m_0^- (y+h^-)}{\cosh m_0^- h^-} + \sum_{k=1}^{N_L} C_k^- e^{m_k^- x} \frac{\cos m_k^- (y+h^-)}{\cos m_k^- h^-} \quad (4.4)$$

although (3.6) is still applicable, viz.,

$$\Phi_S(x, y) = A_0^+ e^{im_0^+ x} \frac{\cosh m_0^+ (y+h^+)}{\cosh m_0^+ h^+} + \sum_{k=1}^{N_R} C_k^+ e^{-m_k^+ x} \frac{\cos m_k^+ (y+h^+)}{\cos m_k^+ h^+} \quad (4.5)$$

Now, because of (4.3) the last integral of (3.4) vanishes. As the analog of (3.11), we obtain the following equation:

$$\begin{aligned} & -\pi\Phi(P) + \int_{S_{0U} S_B} \Phi \frac{\partial}{\partial n} \log r \, ds + \int_{S_F} \Phi \left( \frac{\partial}{\partial n} \log r - \nu \log r \right) ds \\ & + A_0^+ e^{im_0^+ \xi_R} \left( \mathcal{F}_0^+ - iG_0^+ \right) + \sum_{k=1}^{N_R} C_k^+ e^{-m_k^+ \xi_R} \left( \mathcal{F}_k^+ + G_k^+ \right) - A_0^- e^{-im_0^- \xi_L} \left( \mathcal{F}_0^- + iG_0^- \right) \\ & + \sum_{k=1}^{N_L} C_k^- \left( -\mathcal{F}_k^- + G_k^- \right) = -A_I e^{-im_0^- \xi_L} \left( -\mathcal{F}_0^- + iG_0^- \right) \end{aligned} \quad (4.6a)$$

The following equations are the results when the field point P is placed at each junction boundary:

$$\begin{aligned} & \int_{S_{0U} S_B} \Phi \frac{\partial}{\partial n} \log r \, ds + \int_{S_F} \Phi \left( \frac{\partial}{\partial n} \log r - \nu \log r \right) ds \\ & + A_0^+ e^{im_0^+ \xi_R} \left[ -\frac{\pi \cosh m_0^+ (y+h^+)}{\cosh m_0^+ h^+} - iG_0^+(0, y) \right] + \sum_{k=1}^{N_R} C_k^+ e^{-m_k^+ \xi_R} \left[ -\frac{\pi \cos m_k^+ (y+h^+)}{\cos m_k^+ h^+} + G_k^+(0, y) \right] \end{aligned}$$

$$\begin{aligned}
& -A_0^- e^{-im_0^- \xi_L} \left[ \mathcal{F}_0^-(\xi_R - \xi_L, y) + iG_0^-(\xi_R - \xi_L, y) \right] + \sum_{k=1}^{N_L} C_k^- e^{m_k^- \xi_L} \left[ \mathcal{F}_k^-(\xi_R - \xi_L, y) + G_{Tk}^-(\xi_R - \xi_L, y) \right] \\
& = -A_I^- e^{-im_0^- \xi_L} \left[ -\mathcal{F}_0^-(\xi_R - \xi_L, y) + iG_0^-(\xi_R - \xi_L, y) \right] \text{ for } P \in \Sigma_+ \quad (4.6b)
\end{aligned}$$

and

$$\begin{aligned}
& \int_{S_0, S_B} \Phi \frac{\partial}{\partial n} \log r \, ds + \int_{S_F} \Phi \left( \frac{\partial}{\partial n} \log r - \nu \log r \right) ds \\
& + A_0^+ e^{im_0^+ \xi_R} \left[ \mathcal{F}_0^+(\xi_L - \xi_R, y) - iG_0^+(\xi_L - \xi_R, y) \right] + \sum_{k=1}^{N_R} C_k^+ e^{-m_k^+ \xi_R} \left[ \mathcal{F}_k^+(\xi_L - \xi_R, y) + G_{Tk}^+(\xi_L - \xi_R, y) \right] \\
& + A_0^- e^{-im_0^- \xi_L} \left[ -\frac{\pi \cosh m_0^-(y+h^-)}{\cosh m_0^- h^-} - iG_0^-(0, y) \right] + \sum_{k=1}^{N_L} C_k^- e^{m_k^- \xi_L} \left[ -\frac{\pi \cos m_k^-(y+h^-)}{\cos m_k^- h^-} - G_{Tk}^-(0, y) \right] \\
& = A_I^- e^{im_0^- \xi_L} \left[ \frac{\pi \cosh m_0^-(y+h^-)}{\cosh m_0^- h^-} - iG_0^-(0, y) \right] \text{ for } P \in \Sigma_- \quad (4.6c)
\end{aligned}$$

At this point we can proceed to discretize the integral equation as we have previously done for the radiation problems. Once the system of equations is solved, the complex-valued reflection R and transmission coefficient T are simply obtained by

$$R = A_0^- / A_I^-, \quad T = A_0^+ / A_I^+ \quad (4.7)$$

The phase angles are defined by

$$\begin{aligned}
\arg R & \equiv \delta_R = \tan^{-1} \left[ \frac{\text{Im}(R)}{\text{Re}(R)} \right] \\
\arg T & \equiv \delta_T = \tan^{-1} \left[ \frac{\text{Im}(T)}{\text{Re}(T)} \right]
\end{aligned} \quad (4.8)$$

where the arc-tangent is understood to take a range of, i.e.,  $(-\pi, \pi)$ . In this problem, there exist two sets of

reflection and transmission coefficients, corresponding to two different directions of incidence of the propagating waves. The two sets are somewhat related as indicated by Kreisel (1949) and Newman (1965). If we denote  $(R_1, T_1)$ ,  $(R_2, T_2)$  as the reflection and transmission coefficients due to the incidence of the unit-amplitude propagating wave from the left and the right respectively, we can simply write the scattering potential as follows;

$$\varphi_1 \sim \begin{cases} (e^{im_0^-x} + R_1 e^{-im_0^-x}) \chi^-(y) & , x \rightarrow -\infty \\ T_1 e^{im_0^+x} \chi^+(y) & , x \rightarrow +\infty \end{cases} \quad (4.9)$$

and

$$\varphi_2 \sim \begin{cases} (e^{-im_0^+x} + R_2 e^{im_0^+x}) \chi^+(y) & , x \rightarrow +\infty \\ T_2 e^{-im_0^-x} \chi^-(y) & , x \rightarrow -\infty \end{cases} \quad (4.10)$$

where

$$\chi^\pm(y) = \frac{\cosh m_0^\pm (y + h^\pm)}{\cosh m_0^\pm h^\pm}$$

then

$$R_1 = R_2 \quad , \quad R_1 R_1^* + T_1 T_1^* (D^+/D^-) = 1 \quad (4.11)$$

$$\frac{T_1^*}{T_1} = \frac{R_2^*}{R_2} \quad , \quad R_2 R_2^* + T_2 T_2^* (D^-/D^+) = 1$$

$$D^- T_2 = D^+ T_1$$

$$\text{where } D^\pm = \frac{\sinh z m_0^\pm h^\pm + z m_0^\pm h^\pm}{\cosh z m_0^\pm h^\pm + 1} \quad (4.12)$$

and the asteriks indicate complex conjugates. These are useful relations for checking the consistency of the numerical solution.

## VI.2 Relation Between Radiation and Scattering Problems

So far, we have talked about the 'radiation' and 'scattering' problems separately, but we can see that because of the mathematical similarities of these two types of problems, they must be closely related. Certain number of interesting identities have been derived in a recent work by Newman(1975), pertaining to the case of equal asymptotic depth. Yeung(1975) extended results of these identities for the case of unequal depths. The details are reproduced in Appendix B for completeness. The major findings are summarized here. If  $A_{\pm}$ ,  $B_{\pm}$  denote the asymptotic wave-amplitudes of two independent solution of the radiation problem, then

$$\begin{pmatrix} R_1 \\ T_1 \end{pmatrix} = \frac{1}{A_-^* B_+^* - A_+^* B_-^*} \begin{pmatrix} A_+^* B_- - A_- B_+^* \\ (A_- B_-^* - A_+^* B_-) D^- / D^+ \end{pmatrix} \quad (4.13)$$

which can be used to obtain the coefficients  $(R_1, T_1)$ .

$(R_2, T_2)$  then follows from (4.11).

Another useful finding is that Haskind relation which relates the far field behavior of the radiation problem to the exciting force of the scattering problem can be

generalized to the case of unequal depths as follows:

$$F_j^\pm = -\frac{i\rho g}{\sigma^2} D^\pm Y_j^\pm \quad (4.14)$$

where  $F_j^\pm$  is the exciting force or moment in the  $j$ -th direction due to a unit-amplitude incident wave and  $Y_j^\pm$  is the complex-wave amplitude as  $x \rightarrow \pm\infty$  corresponding to the forced oscillation of the body or any part of the bottom contour in the  $j$ -th direction.

## V. RESULTS AND DISCUSSION

The method discussed in section III and IV, has been applied to a number of radiation and scattering problems. In all cases where existing results are available and are known to be correct, the present computation shows very good agreement.

### V.1 Radiation Problems

#### (i) Circular Cylinder in Heave and Sway

The problem of a circular cylinder in heave was first solved by Ursell(1949). It has become a common test problem for newly develop method. Numerical solution for a heaving and sway circular cylinder have been obtained for frequencies,  $K = \frac{\sigma^2}{g} a = 0. \text{ to } 2.0$ , with  $a$  being the radius of the circle, for purpose of comparison with others. Table 1 shows the sway added-mass and damping coefficient (as well as the wave-amplitude ratio) compared with Potash(1970) who used the Havelock wave source to solve the problem. To simulate the infinite-depth situation, we exploit the fact that depth effects for any wave decreases approximately in the form of  $e^{-m_0 h}$ . For a given frequency, we have chosen  $h = 2\lambda = 4\pi/m_0$ . The agreement is clearly assertive of the correctness of the programming efforts.

Results for the heave added-mass and damping coefficients in water of finite but constant depths are shown in

va	$\bar{M}_{11} = \frac{M_{11}}{\rho V}$		$\bar{\lambda}_{11} = \frac{\lambda_{11}}{\rho V \sigma}$		$\bar{A}_{11} = \frac{\text{Wave Amp}}{\text{Motion Amp}}$	
	Kim	Potash	Kim	Potash	Kim	Potash
0.1	1.147	1.156	0.064	0.063	0.031	0.032
0.3	1.282	1.290	0.499	0.501	0.265	0.266
0.4	1.167	1.174	0.716	0.712	0.423	0.426
0.5	0.988	0.993	0.843	0.850	0.574	0.578
0.6	0.810	0.812	0.887	0.895	0.707	0.711
0.7	0.650	0.659	0.877	0.885	0.821	0.825
0.9	0.452	0.450	0.791	0.798	1.003	1.008
1.1	0.335	0.332	0.688	0.695	1.144	1.150
1.3	0.269	0.265	0.597	0.604	1.259	1.266
1.5	0.231	0.226	0.520	0.526	1.356	1.364
1.7	0.211	0.205	0.457	0.462	1.442	1.448
1.9	0.199	0.193	0.405	0.408	1.518	1.521
2.1	0.193	0.187	0.362	0.363	1.585	1.585
2.3	0.190	0.185	0.324	0.324	1.645	1.641
2.5	0.189	0.186	0.291	0.291	1.695	1.691

Number of points on body=19

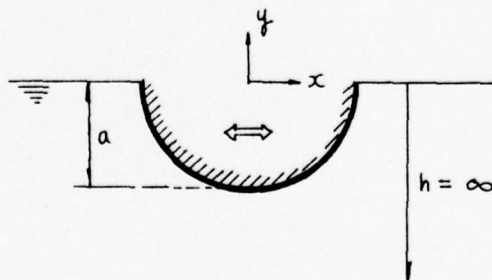
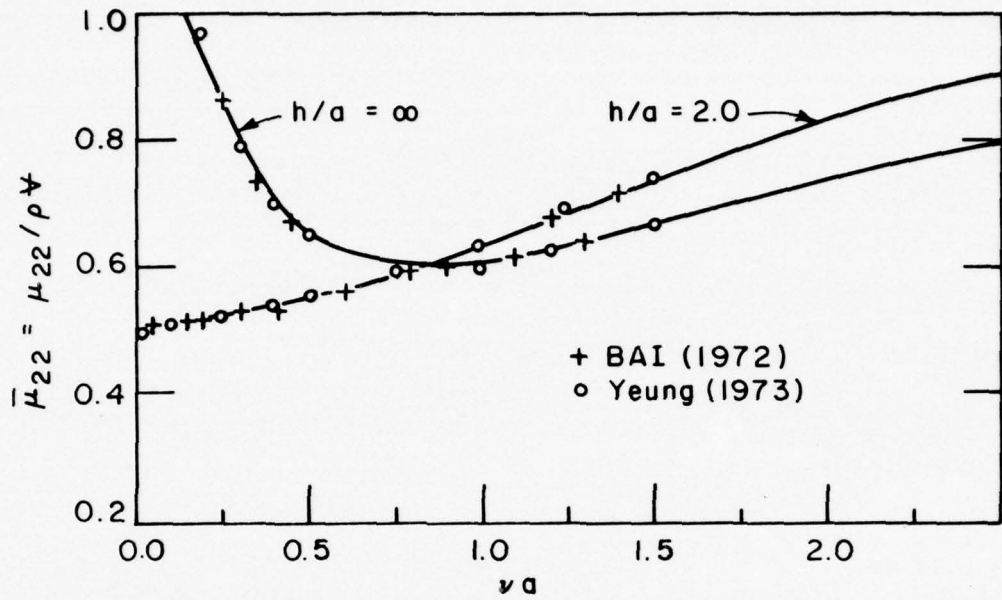


Table 1. Added-Mass, Damping Coefficients and Wave-Amplitude Ratio in Sway Motion



Added - Mass Coefficient in Heave

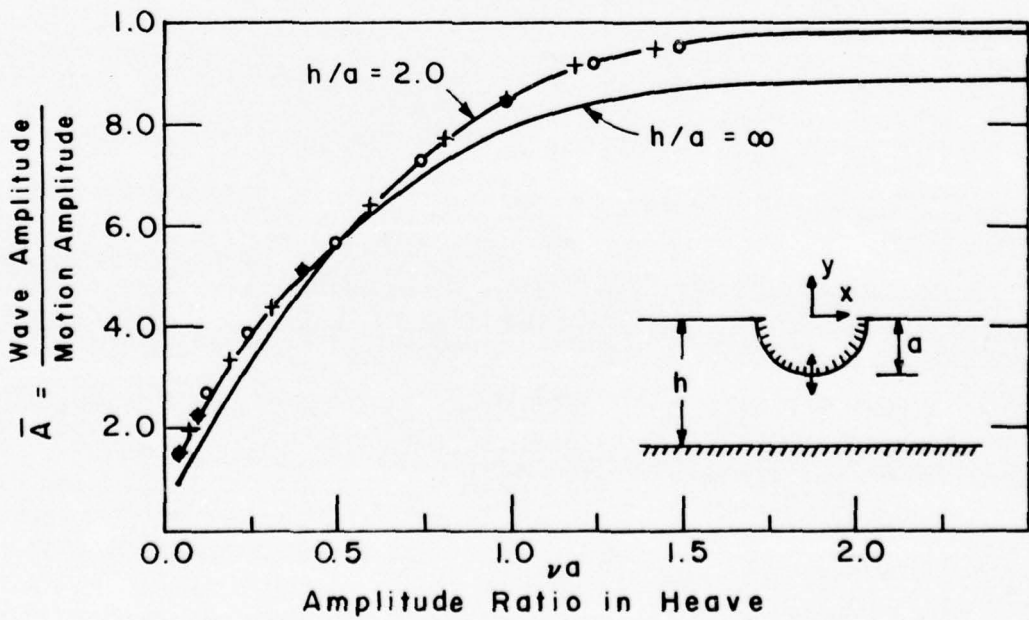


Fig. 3 Added - Mass and Amplitude Ratio for Circular Cylinder in Heave

Figure 3 and compared with Bai and Yeung (1974). In this case,  $h/a=2.0$ . The present calculations yield a value of heave added-mass coefficient equal to 0.500 at  $\nu a=0.001$  which is consistent with the value of 0.4984 obtained by an alternate approach of considering the limiting boundary-value problem (Yeung and Newman, 1976)

Another consistency check consists of the Equation (2.6) relating the local solution obtained by integrating the potential on the body and the far-field wave amplitudes defined by the first term of the eigenfunction expansion Eq. (3.6) and (3.7). For a fluid of unequal depths on each side, this was shown by Yeung (1973) to be

$$\frac{2\sigma^3}{\rho g^2} \lambda_{kk} / \left[ \left| \frac{Y^+}{a} \right|^2 D^+ + \left| \frac{Y^-}{a} \right|^2 D^- \right] = 1 \quad (5.1)$$

This equality is satisfied within 0.5% accuracy in our calculations.

As a gauge on the convergence characteristics of the solution as a function of the location of the radiation boundary, or the number of terms used in the eigenfunction expansions, a small numerical experiment was created and results are summarized in Table 2 for  $\nu a=0.9$  and  $h/a=5.0$ .

The final algorithm developed for the choice of  $\xi_R$  or  $\xi_L$  versus  $N_R$  or  $N_L$  is as follows:

Number of Eigenfunctions = 5

$\xi_R$	$\bar{N}_{22}$	$\bar{\lambda}_{22}$	$\bar{A}$
2.745	0.5937	0.4491	0.7561
3.000	0.5959	0.4490	0.7561
4.500	0.5991	0.4582	0.7642
8.000	0.5996	0.4579	0.7640
15.000	0.5997	0.4578	0.7639

Location of Junction Boundary ( $\xi_R$ ) = 3.0

$N_R$	$\bar{N}_{22}$	$\bar{\lambda}_{22}$	$\bar{A}$
1	0.6448	0.3589	0.6414
3	0.6081	0.4686	0.7780
5	0.5959	0.4490	0.7561
10	0.5961	0.4451	0.7552

Table 2. Summary of Results for Varying the Location of Junction Boundary or the Number of Eigenfunctions

We consider two different cases, one is the uniform depth and the other the varying depth case. For the uniform depth case, in general, taking the junction boundary  $\xi_R$  or  $\xi_L$  as close to the body as possible will reduce the computational time substantially. But in this case, local disturbances play such an important role that a large number of eigenfunctions are required to treat the problem properly. To avoid this deficiency, we usually specify about one-third of a wave-length from the body as an input value of  $\xi_R$  or  $\xi_L$  for each frequency, and 20 is considered as the maximum number of eigenfunctions. As we mentioned in Section III.2, the number

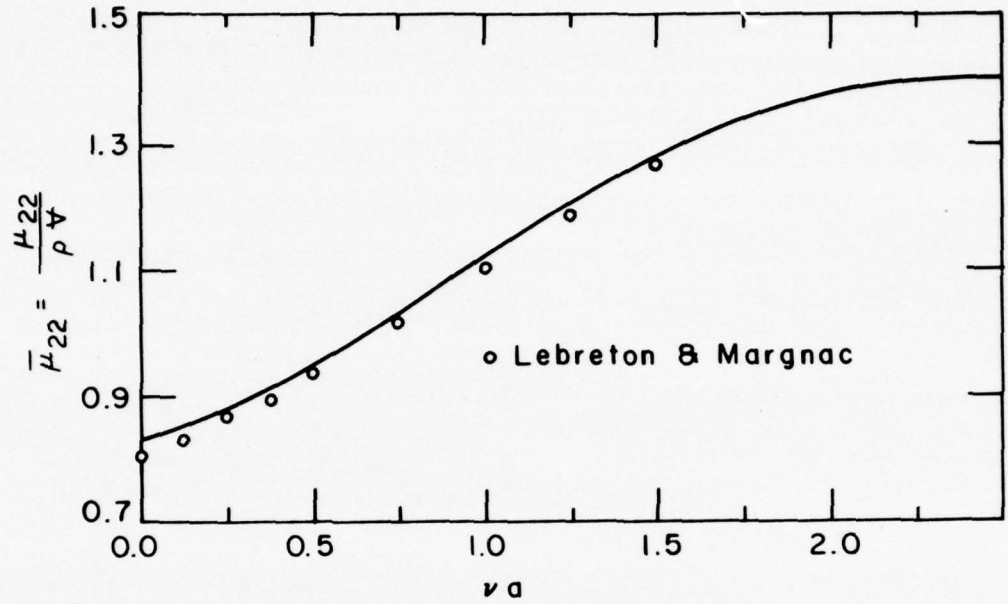
of terms can be less than 20 if the decay factor  $\delta(\kappa, \xi) = e^{-m\kappa\xi}$  satisfies the error criteria before  $N_R$  or  $N_L$  has the value 20. If not, we can change the distance of the junction boundary from the body until the decay factor satisfies the error criteria with  $N_R$  or  $N_L$  set equal to 20. Concerning the varying depth case, we can use exactly the same scheme as the above case except for the initial choice of  $\xi_R$  or  $\xi_L$ .

(ii) Rectangular Cylinder in Heave and Sway

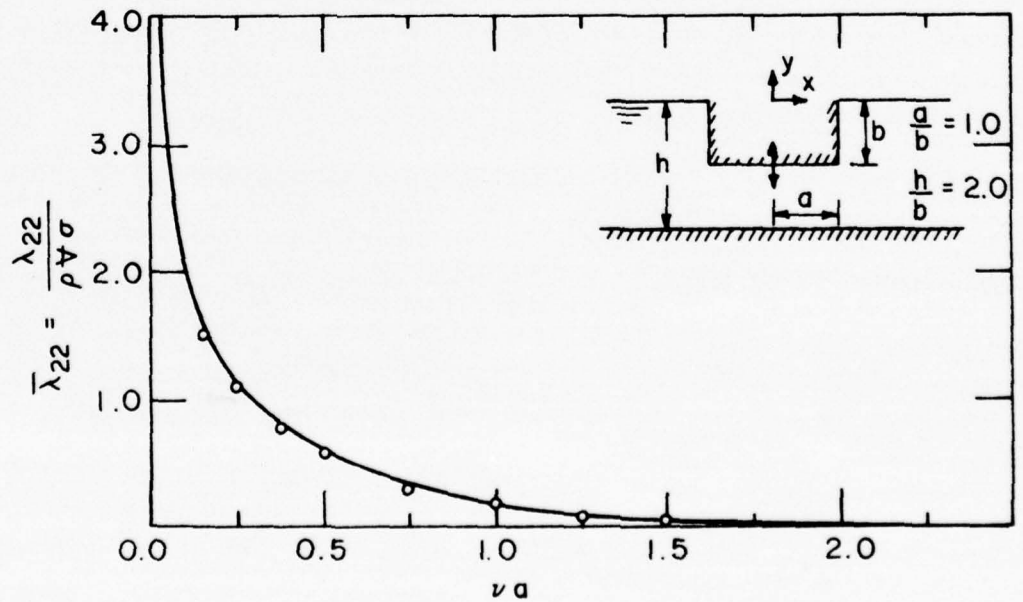
The heave and sway added-mass and damping coefficients in water of finite but constant depth are shown in Figure 4. These results are compared with Lebreton and Margnac (1966) who used the Green-function integral equation technique to solve the problem. The limiting added-mass coefficient is 0.822 as the frequency goes to zero.

(iii) Bulbous Section in Heave or Sway

The bulbous section being considered consists of a fully submerged circle with a narrow vertical stem mounted on top of it as shown in Figure 5. Here, we considered various cases of depth changed,  $h^+ = 1.1d, 1.25d, 1.50d$  and  $2.0d$  holding  $h^- = 2.0d$ . Results for the force coefficients due to sway motion are given in Figure 6.a, and those due to heave motion, in Figure 6.b. It is of interest to note that for the heave motion, the added-mass coefficients



Added - Mass Coefficient in Heave



Damping Coefficient in Heave

Fig. 4 Added - Mass and Damping Coefficient for Rectangular Cylinders in Heave

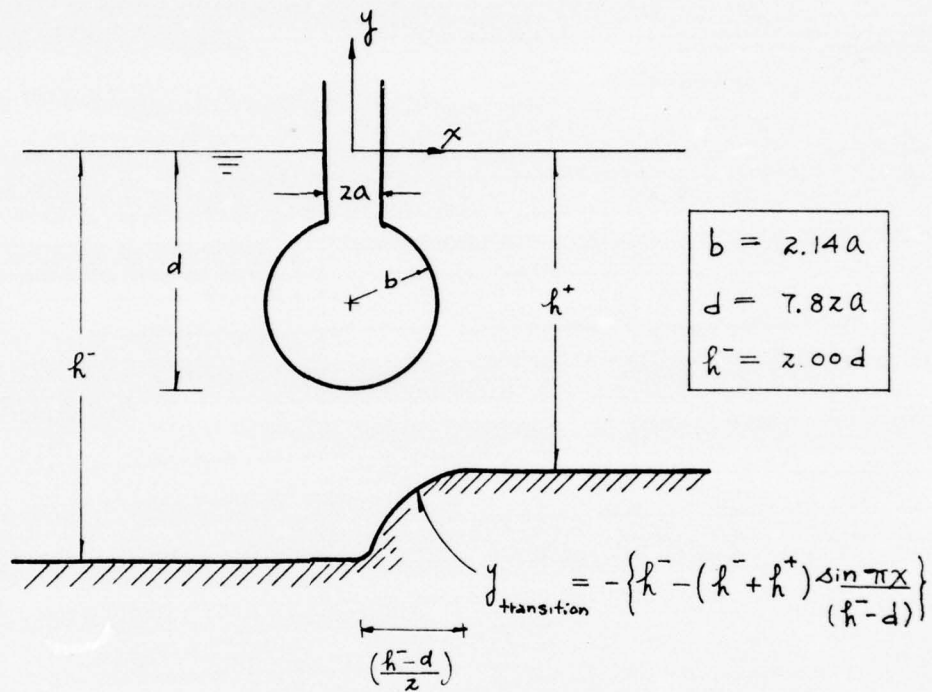


Fig. 5 Bottom Geometry with Bulbous Section

increase proportionally to a decrease of depth throughout most of the frequency range, but the damping coefficients remain practically the same, especially when  $\nu a \geq 0.15$ . On the other hand, hydrodynamic coefficients associated with sway mode behave differently. In all cases, when  $\nu a \geq 0.20$  coefficients are almost identical. One phenomenon we notice is that in some frequency range the sway added-masses become vanishingly small and even slightly negative. Such an occurrence of negative sway added-mass observed by Ogilvie (1963) when a fully submerged circular cylinder undergoes sway.

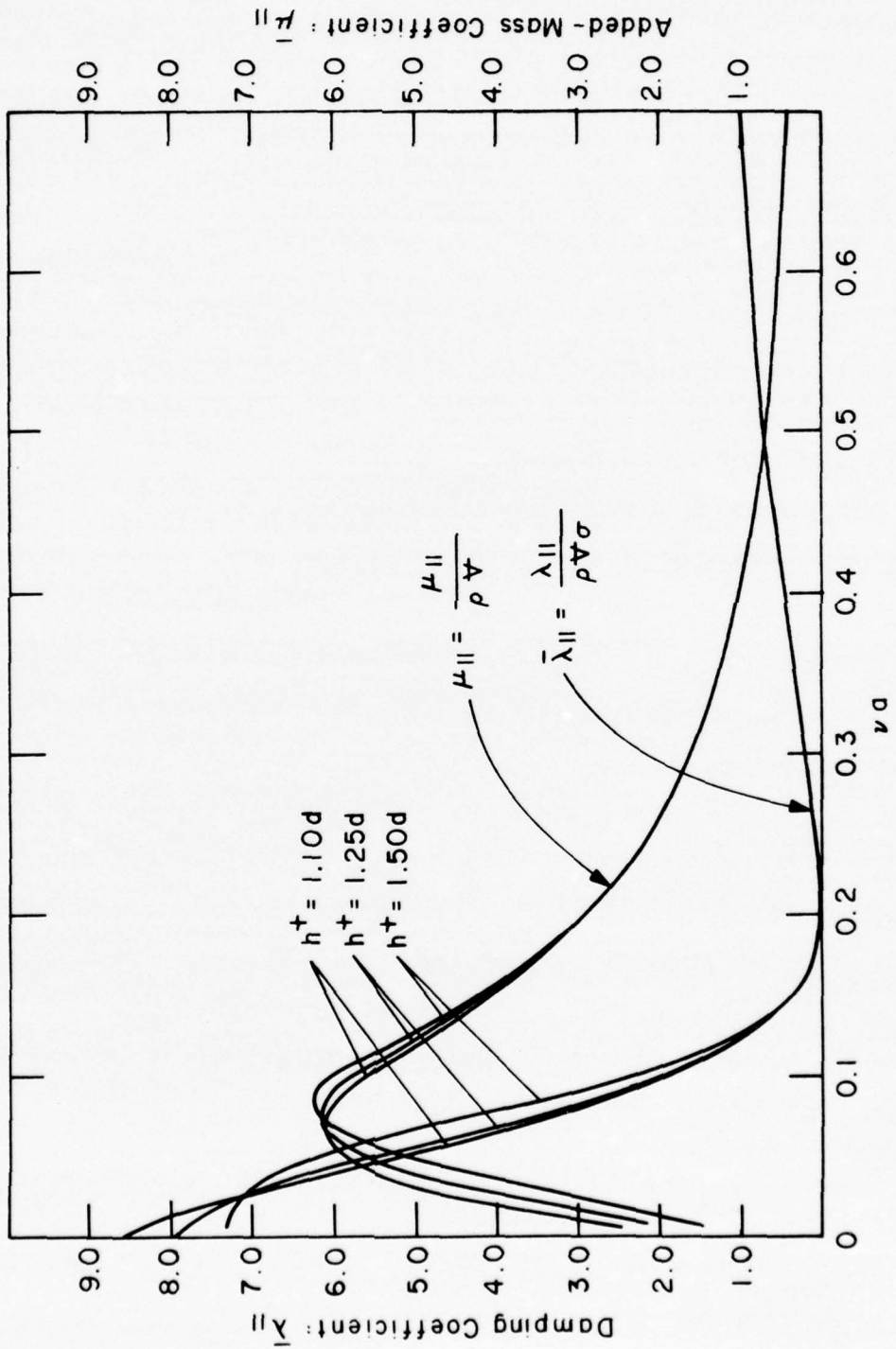


Fig. 6a Added - Mass and Damping Coefficient for Bulbous Section in Sway

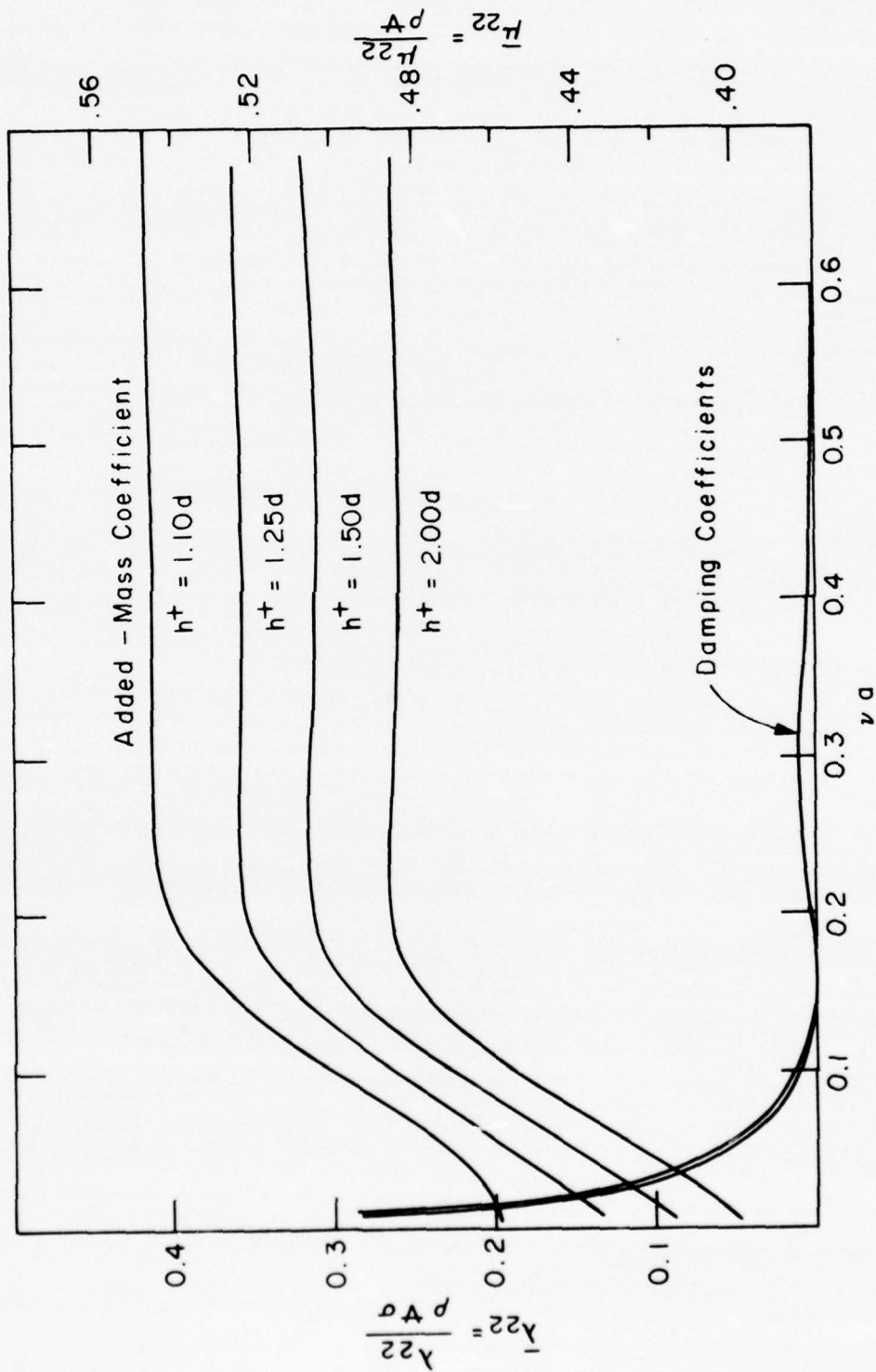


Fig. 6b Hydrodynamic Coefficients for Bulbous Section in Heave

## V.2 Scattering Problems

### (i) Sinusoidal Hump

The geometry and results are shown in Figure 7.  $Y_T(x)$  is the total wave-amplitude function due to an incident wave of unit amplitude propagating from the left over the sinusoidal hump. The results obtained here show very good agreement with Bai(1972) obtained using a finite element method. The complex wave-function  $Y_T(x)$  is defined as

$$Y_T(x) = e^{im_0x} + Y_D(x) = Y_1(x) + iY_2(x) \quad (5.2)$$

where the first term after the first equal sign represents the incident wave with unit-amplitude and the second the diffracted wave profile. This test essentially verifies our theory discussed in Section IV.1 for the treatment of the scattering problem.

### (ii) Finite-Size Step

The reflection and transmission coefficients of a finite-size step are given in Table 3 and 4, and compared with Hilaly(1967) for  $h^-/h^+ = 2.5$  and  $6.5$ . From equation (4.8) and (4.11), we expect

$$|R_1| = |R_2| \quad (5.3)$$

$$|R_1|^2 + |T_1|^2 (D^+/D^-) = 1. \quad (5.4)$$

where  $(R_1, T_1)$  and  $(R_2, T_2)$  are the resulting reflection and

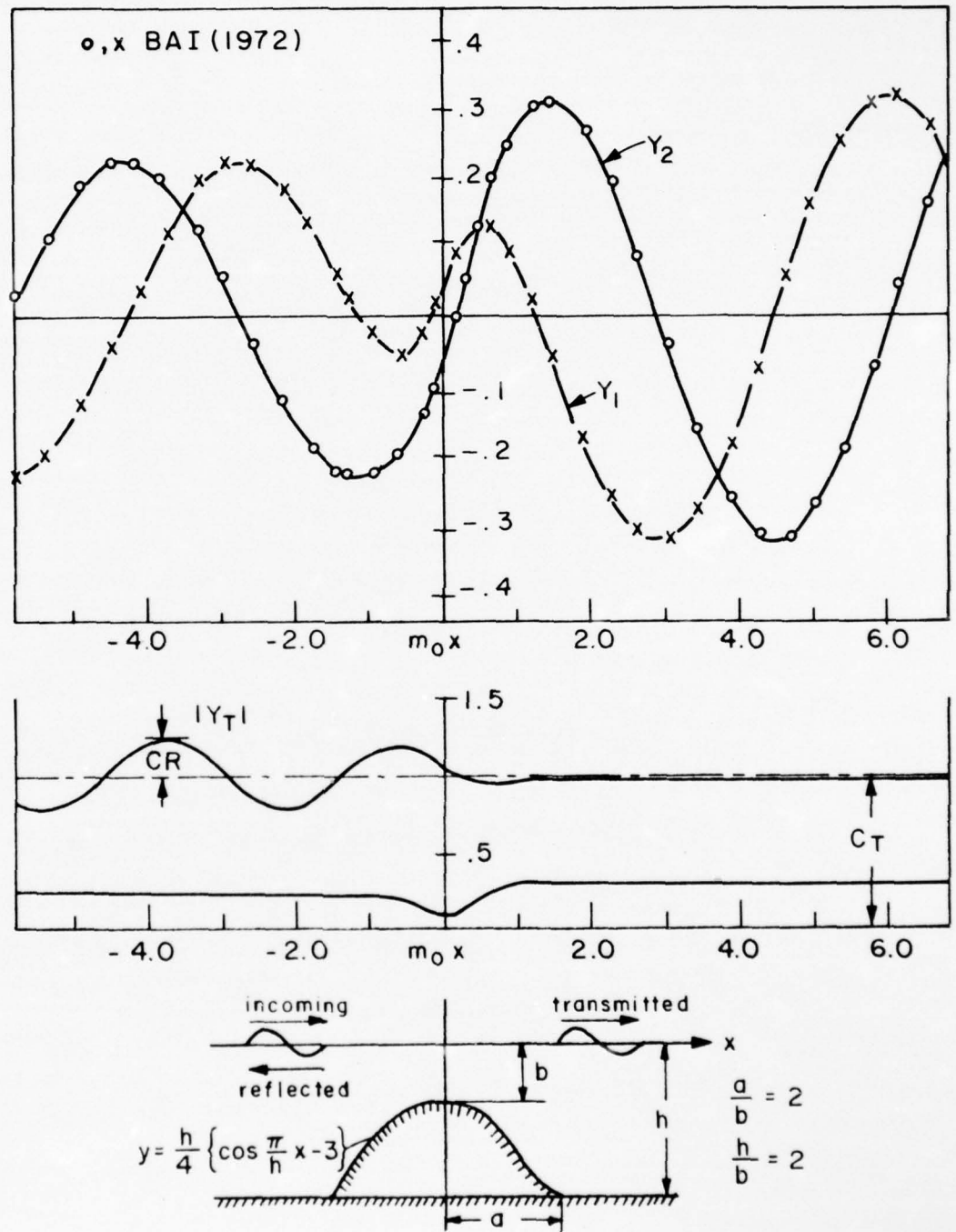


Fig. 7 Scattering Wave over Sinusoidal Hump

$\nu h^-$	$R_1$		$T_1$		Eqn (5.4)
	$ R_1 $	$\arg R_1 (^\circ)$	$ T_1 $	$\arg T_1 (^\circ)$	L.H.S. <del>of</del>
0.03395	0.4269	-163.14	0.5799	4.99	1.00025
	0.4273*	-163.26*	0.5797*	4.97*	1.00001
0.04365	0.4242	-160.86	0.5846	5.64	1.00016
	0.4246	-161.00	0.5846	5.61	1.00001
0.05813	0.4201	-157.86	0.5918	6.46	1.00011
	0.4205	-158.02	0.5917	6.44	1.00005
0.06644	0.4134	-153.73	0.6035	7.56	1.00002
	0.4138	-153.93	0.6034	7.53	1.00007
0.12115	0.4016	-147.68	0.6244	9.04	0.99980
	0.4021	-147.94	0.6244	9.02	1.00008
0.20031	0.3774	-137.97	0.6679	11.07	0.99938
0.39260	0.3158	-120.25	0.7803	13.05	0.99851
	0.3162	-120.83	0.7810	13.03	1.00023
1.09093	0.1458	-90.67	1.0395	7.61	0.99760
	0.1470	-91.99	1.0407	7.69	1.00025

\* Taken from Hilaly (1967). His phase angle is related to the present notation by:  $\alpha = -(\pi + \arg R)$

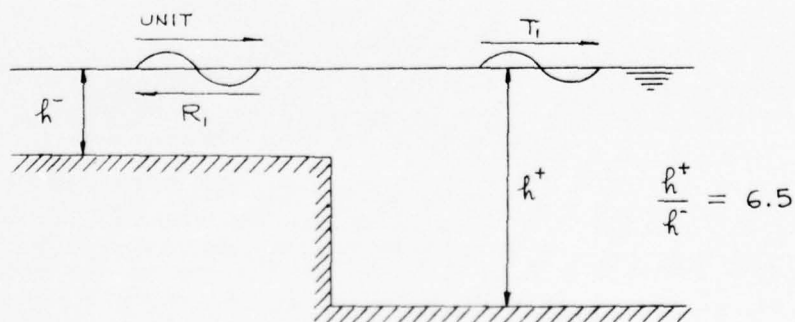
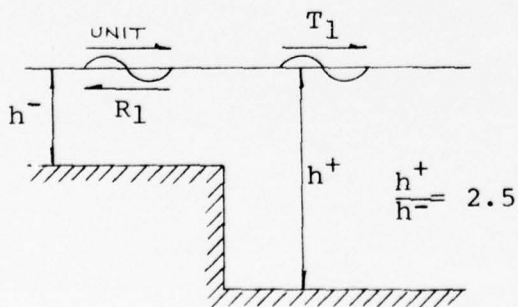


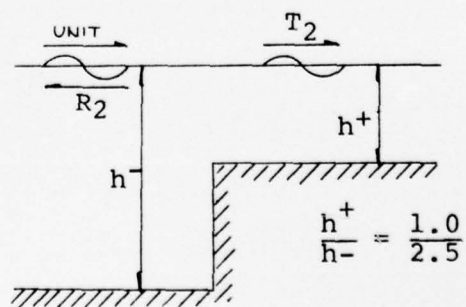
Table 3. Reflection and Transmission Coefficients of a Step

$\nu (= \frac{\sigma^2}{g})$	CASE I				CASE II			
	$R_1$	arg $R_1$	$T_1$	arg $T_1$	$R_2$	arg $R_2$	$T_2$	arg $T_2$
.0170	.2212	-170.6	.7820	1.65	.2217	-6.12	1.216	1.65
	.223*	-170.7*	.7802*	1.66*				
.0218	.2206	-169.3	.7835	1.86	.2205	-6.96	1.214	1.86
	.2223	-169.4	.7818	1.88				
.0291	.2196	-167.6	.7858	2.14	.2196	-8.07	1.211	2.15
	.2213	-167.8	.7841	2.17				
.0406	.2181	-165.3	.7895	2.52	.2182	-9.61	1.206	2.52
	.2198	-165.5	.7878	2.56				
.0606	.2154	-162.0	.7960	3.05	.2154	-11.9	1.198	3.05
	.2170	-162.3	.7944	3.01				
.1003	.2100	-156.6	.8091	3.85	.2100	-15.7	1.182	3.84
	.2114	-157.0	.8076	3.91				
.1965	.1964	-146.5	.8421	5.08	.1964	-23.4	1.142	5.08
	.1973	-147.1	.8410	5.18				
.5459	.1423	-120.0	.9657	5.91	.1423	-48.1	1.015	5.91
	.1413	-121.1	.9654	6.07				

\* Taken from Hilaly. His phase angle is related to the present notation by:  $\alpha = -(\pi + \arg R)$



(Case I)



(Case II)

Table 4. Comparison of Reflection and Transmission Coefficients for Incident Waves in Opposite Directions

transmission coefficients when an incident wave of unit-amplitude comes from the left and right respectively. The ratio  $D^+/D^-$  evidently represents the group-velocity ratio. The phase angles given in these tables are defined by (4.8). Our results not only show very good agreement with Hilaly's, but also meet the testing of Equation (5.3) and (5.4) with sufficient accuracy.

(iii) Steep Hump at a Step

We apply our numerical method to determine the reflection ability of a steep hump located in front of a step. This is one sample of physical geometry which can not be easily accommodated by any analytical methods. The geometry of the hump and the results are presented in Figure 8. From Equation (4.11) one can define an energy transmission factor  $\kappa$  by  $\kappa = |T|^2 D^+/D^-$ . The hydrodynamic characteristics, reflection and transmission coefficients, associated with a finite-size step without the hump (Table 4) are also plotted for the purpose of comparison. One notices that the hump causes a considerable increase in wave reflection, and the energy transmission factor achieves a minimum at a frequency of  $\nu h^- = 1.0$ .

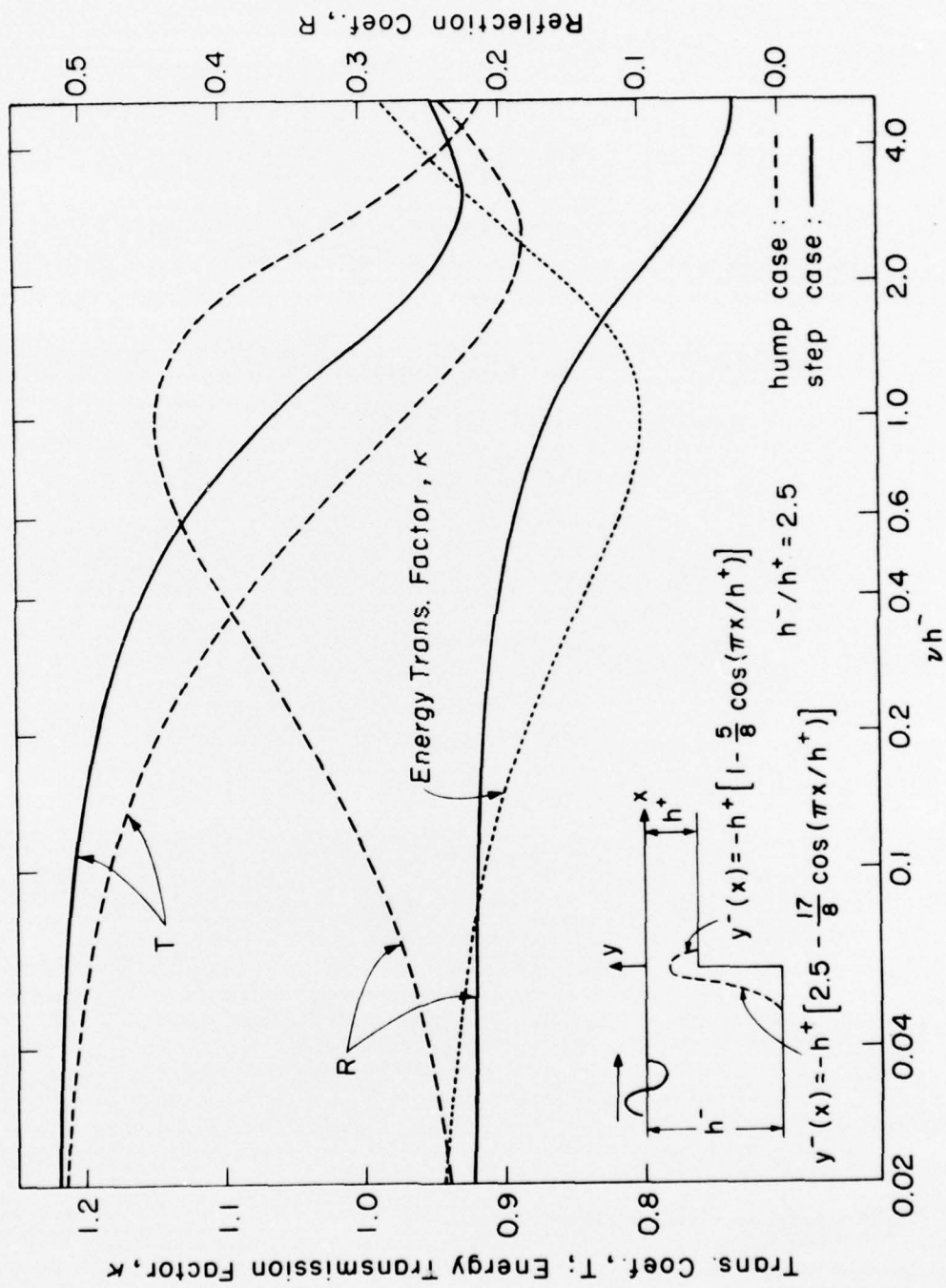


Fig. 8 Reflection and Transmission Coeffs. of a hump

## VI. REMARKS

In this thesis, we have presented a versatile numerical method of solution which is applicable to the two-dimensional time-harmonic free-surface flow problem for a fluid of arbitrary bottom topography and have investigated the validity of this method by comparing our results with others known to be correct. In every case, we obtained very satisfactory agreement. One item we should mention is that for scattering problems the numerical accuracy is not as good as expected when the reflection coefficient becomes vanishingly small as the frequency becomes fairly high. To avoid this deficiency, it seems to be worthwhile to make a modification in computational procedure. It is possible to extend this method to a general three-dimensional problem without any appreciable amount of conceptual difficulties.

#### REFERENCES

1. Abramowitz, M. & Stegun, I.A.  
Handbook of Mathematical Function, Dover Publications,  
New York, 1976, xiv+1046p
2. Bai, K.J.  
'A Variational Method in Potential Flows with a Free  
Surface,' Univ. of Calif. Berkeley, College of Eng'g,  
Rep.NA 72-2, Sept. 1972, vi+137p
3. Bai, K.J. & Yeung, R.W.  
'Numerical Solutions to Free-Surface Flow Problems,'  
*10th Symp. on Naval Hydrodynamics*, Cambridge, MA 1974
4. Evans, D.V.  
'The Application of a New Source Potential to the Problem  
of the Transmission of Water Waves over a Shelf of Arbitrary  
Profile,' *Proc. Camb. Phil. Soc.*, vol. 71, 1972, 391-410p
5. Frank, W.  
'Oscillation of Cylinders in or below the Free Surface  
of Deep Fluids,' Naval Ship Research and Development  
Center, Report 2375, 1967, vi+40p
6. Grim, O.  
'Berechnung der durch Schwingungen einen Schiffskoerpers  
Erzeugren Hydrodynamischen Kraefte,' *Jahrbuch der Schiffe-  
bautechnischen Gesellschaft*, Vol. 47, 1953, 277-299p
7. Hilaly, N.  
'Diffraction of Water Waves over Bottom Discontinuities,'  
Univ. of Calif. Berkeley, Rept.HEL 1-7, Sep. 1967, 142p
8. Lebreton, J.C. & Margnac, M.A.  
'Traitement sur Ordinateur de Quelques Problems Concer-  
nant l'Action de la Houle sur Corps Flottants en Theorie  
Bidimensionelle,' *Bulletin du Centre de Recherches et d'essaus  
de Chatou*, No. 18, 1966
9. Miles, J.W.  
'Surface-Wave Scattering Matrix for Shelf,' *J. Fluid Mech.*,  
vol. 28, 1967, 755-756p
10. Newman, J.N.  
'Propagation of Water Waves over an Infinite Step,'  
*J. Fluid Mech.*, vol. 23, 1965, 399-415p

11. Newman, J. N.  
'Interaction of Waves with Two-dimensional Obstacles:  
a Relation between the Radiation and Scattering Problems,'  
*J. Fluid Mech.*, vol 71, 1975, 273-282 p.
12. Ogilvie, T. F.  
'First-and Second-Order Forces on a Cylinder Submerged under  
a Free Surface,' *J. Fluid Mech.*, vol 16, 1963, 451-472 p.
13. Porter, W. R.  
'Pressure Distribution, Added Mass and Damping Coefficients  
for Cylinder Oscillating in a Free Surface,' *Inst. Eng'g  
Res.*, Univ. of Calif. Berkeley, Series 82, Issue 16, 1960  
x + 181 p.
14. Potash, R. L.  
'Second-Order Theory of Oscillating Cylinders,' *J. Ship Research*,  
vol 15, 1971, 295-324 p.
15. Szegő, C.  
Orthogonal Polynomials, Amer. Math. Soc. Coll. Publication  
23, 1939, 369 p.
16. Tasai, F.  
'On the Damping Force and Added Mass of Ships Heaving and  
Pitching,' *J. Zosen Kiokai*, vol 105, 1959, 47-56 p.
17. Todd, J.  
'Evaluation of the Exponential Integrals for Large Complex  
Argument,' *J. Research of the National Bureau of Standard*,  
vol 52, June 1954, 313-317 p.
18. Ursell, F.  
'On the Heaving Motion of a Circular Cylinder in the  
Free Surface of a Fluid,' *Quart. J. Mech. Appl. Math.*,  
vol 2, 1949, 218-231 p.
19. Wehausen, J. V. & Laitone, E. V.  
'Surface Waves,' *Handbuch der Physik*, vol 9, Springer-  
Verlag, Berlin, 1960, 446-778 p.
20. Yeung, R. W.  
'A Singularity-Distribution Method for Free-Surface Flow  
Problems with an Oscillating Body,' Univ. of Calif. Ber-  
keley, College of Eng'g, Report NA 73-6, 1973, vi + 124 p.
21. Yeung, R. W. & Newman, J. N.  
'On the Low-frequency Limit of Added Mass of Cylinders,'  
written discussion, Session V, 11th Symp. on Naval Hydro.,  
London, 1976.
22. Yeung, R. W.  
'A Hybrid Integral-Equation Method for Time-Harmonic Free-  
Surface Flow,' *Proceedings of the 1st Int. Conf. on Numerical Ship  
Hydro.*, Gaithersburg, Oct, 1976, pp. 581-607

APPENDIX A

The Integrals  $\mathcal{F}_k$  and  $G_k$

Consider the integrals  $\mathcal{F}$  and  $G$  proportional to those defined by (3.10):

$$\begin{aligned} \mathcal{F}(x-\xi, y) \\ G(x-\xi, y) \end{aligned} = \int_{-k}^0 d\eta \cos m(\eta+k) \left\{ \begin{array}{l} -\frac{\partial}{\partial x} \log r \\ m \log r \end{array} \right\} \quad (\text{A.1})$$

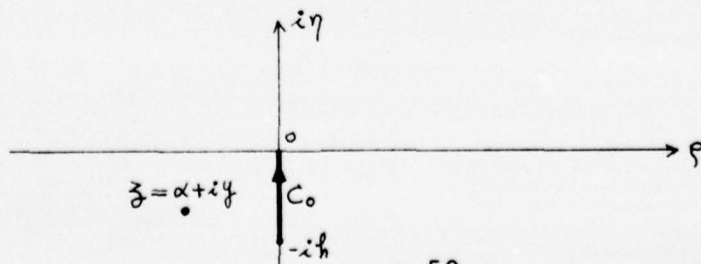
We will show that they can be written in terms of exponential integrals. The derivation to follow is considerably simpler if we introduce the following complex variables:

$$\begin{aligned} \tilde{z} &= \alpha + iy, \quad \alpha = x - \xi \\ \zeta &= \rho + i\eta \end{aligned}$$

where for practical purposes one only has to consider the case  $(x-\xi) < 0$  since  $G$  remains the same while  $\mathcal{F}$  differs only by a sign for the opposite case. In the complex plane  $G(z)$  is given by:

$$\begin{aligned} G(\alpha-y) &= \text{Re} \left\{ -i \int_{C_0} d\zeta \cosh m(\zeta+ik) m \log(\tilde{z}-\zeta) \right\} \\ &\equiv \text{Re} \{ W(\tilde{z}) \} \end{aligned} \quad (\text{A.2})$$

where the contour of integration  $C_0$  is a vertical line from  $\zeta = -ik$  to  $\zeta = 0$  as shown in Fig. A.1.



If  $W(z)$  is known, the evaluation of  $\mathcal{F}$  is straightforward since

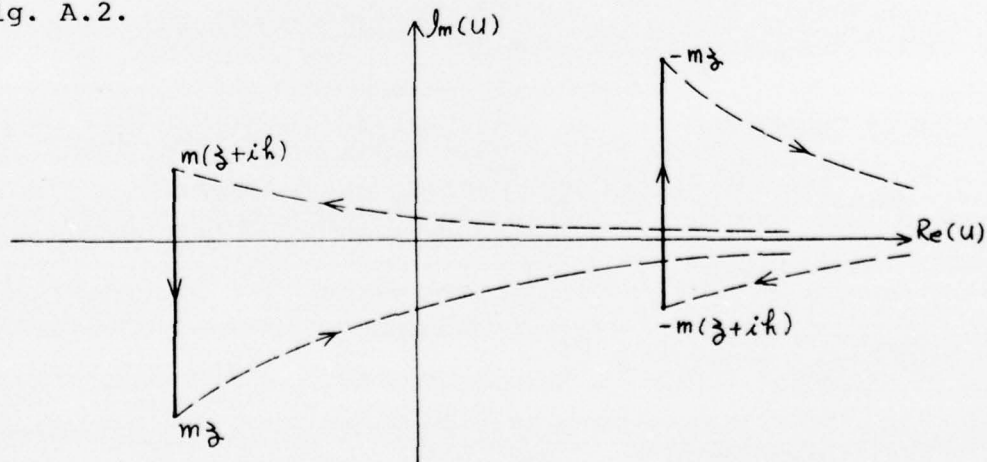
$$\mathcal{F}(\alpha, y) = \frac{-1}{m} \operatorname{Re} \left\{ \frac{d}{dz} G(\bar{z}) \right\} \quad (\text{A.3})$$

which follows from the fact that the derivative of any analytic function is independent of the direction of approach.

Now for  $W(z)$ , an integration by parts yields

$$\begin{aligned} W(\bar{z}) &= -i \left\{ \sinh(imh) \log \bar{z} + \int_{c_0} \frac{\sinh m(\zeta + ih)}{\bar{z} - \zeta} d\zeta \right\} \\ &= i \left\{ \sinh(imh) \log \bar{z} + \frac{1}{z} e^{m(\zeta + ih)} \int_{m(\zeta + ih)}^{m\bar{z}} \frac{e^{-u}}{u} du \right. \\ &\quad \left. + \frac{1}{z} e^{-m(\bar{z} + ih)} \int_{-m(\bar{z} + ih)}^{-m\bar{z}} \frac{e^{-u}}{u} du \right\} \end{aligned} \quad (\text{A.4})$$

The paths of the integrals of (A.4) in the  $u$ -plane are shown in Fig. A.2.



Both integrals can be replaced by a pair of integrals extending from the end points to  $z = +\infty$ . Exploiting the definition of the exponential integral  $E_1(z)$

$$E_1(z) = \int_z^\infty \frac{e^{-t}}{t} dt, \quad |\arg z| < \pi \quad (\text{A.5})$$

where the Riemann cut is along the negative real axis, we obtain for (A.4), after accounting for the pole at  $u=0$  for the first integral, the following expression:

$$W(z) = i \left\{ \sinh(imh) + \frac{1}{2} e^{m(z+ik)} \left[ -E_1(mz) + E_1(m(z+ik)) + 2\pi \right] \right. \\ \left. + \frac{1}{2} e^{-m(z+ik)} \left[ -E_1(-mz) + E_1(-m(z+ik)) \right] \right\} \quad (\text{A.6})$$

Whence,

$$G(\alpha, y) = \sin mh \log(\alpha^2 + y^2)^{\frac{1}{2}} - \pi \cos m(y+h) e^{m\alpha} \\ + \frac{1}{2} \text{Im} \left\{ e^{m(z+ik)} \left[ E_1(mz) - E_1(m(z+ik)) \right] \right. \\ \left. - e^{-m(z+ik)} \left[ E_1(-mz) - E_1(-m(z+ik)) \right] \right\} \quad (\text{A.7})$$

which is (3.27). Next for  $\mathcal{F}(\alpha, y)$ , we recall that by Liebnitz rule

$$\frac{d}{d\alpha} e^{\alpha} E_1(\alpha) = e^{\alpha} E_1(\alpha) - \frac{1}{\alpha} \quad (\text{A.8})$$

Using (A.3) and (A.6), we have for the normal-derivative integral:

$$\mathcal{F}(\alpha, y) = -\pi \text{sgn}(\alpha) e^{-m(\alpha)} \cos m(y+h) \\ + \frac{1}{2} \text{Im} \left\{ e^{m(z+ik)} \left[ E_1(m(z+ik)) - E_1(mz) \right] \right\}$$

$$+ e^{-m(z+ik)} \{ E_1(-m(z+ik)) - E_1(-mz) \} \quad (\text{A.9})$$

which is identical to that indicated in (3.26). Note that as  $\alpha \rightarrow 0$  the exponential-integral terms vanish in pairs because

$$E_1(z^*) = [E_1(z)]^* \quad (\text{A.10})$$

and (A.9) reduces to merely

$$\mathcal{F}(0^\pm, y) = -\pi \operatorname{sgn}(\alpha) \cos m(y+k). \quad (\text{A.11})$$

which follows naturally from the physical interpretation of the integral as the normal velocity of a source-distribution. In this same limit,  $G(\alpha, y)$  can be written as the sine- and cosine-integrals:

$$\begin{aligned} G(0, y) = & \sin mh \log |y| + \sin m(y+k) [C_i(m(y+k)) - C_i(-my)] \\ & - \cos m(y+k) [S_i(m(y+k)) - S_i(-my)] \end{aligned} \quad (\text{A.12})$$

where  $C_i$  and  $S_i$  are those defined in Abramowitz and Stegun (1970).

APPENDIX B

Symmetry Relations for Radiation and Scattering Problems

Let  $\varphi_1$  and  $\varphi_2$  be the spatial scattering potentials corresponding to a unit amplitude right- or left-moving incident wave respectively. Therefore asymptotically

$$\varphi_1 \sim \begin{cases} [e^{im_0^-x} + R_1 e^{-im_0^-x}] \chi^-(y), & x \rightarrow -\infty \\ T_1 e^{im_0^+x} \chi^+(y), & x \rightarrow +\infty \end{cases} \quad (\text{B.1})$$

and

$$\varphi_2 \sim \begin{cases} [e^{-im_0^+x} + R_2 e^{im_0^+x}] \chi^+(y), & x \rightarrow +\infty \\ T_2 e^{-im_0^-x} \chi^-(y), & x \rightarrow -\infty \end{cases} \quad (\text{B.2})$$

where the R's and T's are complex-valued transmission and reflection coefficients.

Next, define the integral operator  $\langle \varphi, \psi \rangle$  on two potential functions  $\varphi$  and  $\psi$  as

$$\langle \varphi, \psi \rangle = \int_C [\varphi \psi_n - \psi \varphi_n] ds \quad (\text{B.3})$$

where C consists of the boundary contours  $S_F$ ,  $S_B$ ,  $S_O$ , and two vertical boundaries at infinities. Making use of the boundary conditions (2.3b), (2.3c), and (4.3) as well as the asymptotic behavior of  $\varphi_1$  and  $\varphi_2$ , we have

$$\langle \varphi_1, \varphi_1^* \rangle: 1 = R_1 R_1^* + (T_1 T_1^*) \frac{D^+}{D^-} \quad (\text{B.4})$$

$$\langle \Phi_2, \Phi_2^* \rangle: 1 = R_2 R_2^* + (T_2 T_2^*) D^- / D^+ \quad (\text{B.5})$$

$$\langle \Phi_1, \Phi_2 \rangle: T_2 D^- = T_1 D^+ \quad (\text{B.6})$$

$$\langle \Phi_1, \Phi_2^* \rangle: T_2^* R_1 D^- = -T_1 R_2^* D^+ \quad (\text{B.7})$$

where  $D^\pm (m_0^\pm h^\pm)$  is defined earlier by (2.18). The first two equations are statements of conservation of energy. Together with (B.6), one can deduce easily that

$$|R_1| = |R_2| \quad (\text{B.8})$$

(B.7) and (B.8) can also be combined to yield

$$\frac{T_1^*}{T_1} = \frac{R_2^*}{R_1} \quad (\text{B.9})$$

Hence if  $T_1$  and  $R_1$  are known, (B.6), (B.8), and (B.9) define  $R_2$  and  $T_2$  completely. These are essentially restatements of observation by Kreisel (1949) and Newman (1965). We reproduce them here for the sake of completeness.

To obtain relations between the radiation problems and scattering problems, we denote the radiation potential by  $\varphi$ , which has an asymptotic behavior of

$$\varphi \sim \begin{cases} A_+ \chi^+(y) e^{i m_0^+ x} \\ A_- \chi^-(y) e^{-i m_0^- x} \end{cases} \quad \text{as } \begin{cases} x \rightarrow +\infty \\ x \rightarrow -\infty \end{cases} \quad (\text{B.10})$$

and boundary condition on  $S_0$  defined by (2.3d). Now applying

the operator (B.3) to the following combination of  $\varphi$  and  $\varphi_1$ , or  $\varphi_2$  we have

$$\langle \varphi_1, \varphi^* \rangle: \bar{D}A_-^* R_1 + D^+ A_+^* T_1 + i \oint_{S_0} \varphi_1 f^*(s) ds = 0 \quad (\text{B.11})$$

$$\langle \varphi_1, \varphi \rangle: \bar{D}A_- - i \oint_{S_0} \varphi_1 f(s) ds = 0 \quad (\text{B.12})$$

$$\langle \varphi_2^*, \varphi \rangle: \bar{D}A_- T_2^* + D^+ A_+ R_2^* - i \oint_{S_0} \varphi_2^* f(s) ds = 0 \quad (\text{B.13})$$

$$\langle \varphi_2, \varphi \rangle: D^+ A_+ - i \oint_{S_0} \varphi_2 f(s) ds = 0 \quad (\text{B.14})$$

This basically covers all possible combinations. Note that (B.12) and (B.14) are essentially Haskind relations for the unequal depth case; namely if  $F_j$  denotes the excitation force or moment on the body  $S_0$  in the  $j$ -th direction due to unit-amplitude incident wave then

$$F_j^\pm = \frac{-i \rho g^2}{\sigma^2} D^\pm (mk) Y_0^\pm \quad (\text{B.15})$$

where  $Y_0^\pm$  are the asymptotic wave amplitude of  $\varphi$  with a boundary conditions  $f(s)$  corresponding to a unit oscillation of the  $j$ -th mode. (B.11) and (B.12) can be combined together noting that  $f(s)$  is real for radiation problems; whence

$$\bar{D}A_-^* R_1 + D^+ A_+^* T_1 + \bar{D}A_- = 0 \quad (\text{B.16})$$

Similarity, for (B.13) and (B.14)

$$\bar{D}A_- T_2^* + D^+ A_+ R_2^* + D^+ A_+ = 0 \quad (\text{B.17})$$

It is not obvious that (B.17) is a redundant relation. To show this, we multiply (B.16) by  $R_1^*$  and add the result to itself,

$$\bar{D}A_-^* R_1^2 + D^+ A_+^* T_1 R_1^* - D^+ A_+ T_1^* - \bar{D}A_-^* = 0 \quad (\text{B.18})$$

Next, making use of (B.4) for the first term we have

$$\left[ -D^+ A_-^* T_1 + D^+ A_+^* \frac{T_1 R_1^*}{T_1^*} - D^+ A_+ \right] T_1^* = 0 \quad (\text{B.19})$$

Hence by (B.6) and (B.9), we recover (B.16). Therefore, as in the constant depth case, only one equation is available. But unlike the case considered by Newman (1975), because of the bottom geometry, a symmetrical body will not necessarily generate symmetric or anti-symmetrical wave motion. Similar simplifications do not result. On the other hand, deduction of the value of transmission and reflection coefficients from the radiation problem is still possible.

Denote the modified wave amplitude at infinities of two modes of oscillations by  $\tilde{A}_\pm$ ,  $\tilde{B}_\pm$ , then

$$\begin{aligned} \tilde{A}_\pm &= D^\pm Y_A^\pm \\ \tilde{B}_\pm &= D^\pm Y_B^\pm \end{aligned} \quad (\text{B.20})$$

where  $Y_A^\pm$ ,  $Y_B^\pm$  are the complex spatial wave amplitude defined by (2.8d) with  $|a| = 1.0$ . Straightforward application of

(B.16) twice then yields

$$\begin{bmatrix} R_1 \\ T_1 \end{bmatrix} = \frac{1}{(\tilde{A}_- \tilde{B}_+^* - \tilde{A}_+^* \tilde{B}_-)} \begin{bmatrix} \tilde{A}_+^* \tilde{B}_- - \tilde{A}_- \tilde{B}_+^* \\ \tilde{A}_- \tilde{B}_-^* - \tilde{A}_+^* \tilde{B}_- \end{bmatrix} \quad (\text{B.21})$$

$R_2, T_2$  are then given by (B.6), (B.8), and (B.9). Alternatively, one may obtain  $R_2, T_2$  in terms of  $\tilde{A}_\pm$  and  $\tilde{B}_\pm$  by using (B.17).